

DOE/NASA/3230-1
NASA CR-165324

NASA-CR-165324
19820005634

Transient Catalytic Combustor Model

James S. T'ien
Case Western Reserve University

May 1981

LIBRARY COPY

FEB 5 1982

LANGLEY RESEARCH CENTER
LIBRARY, NASA
HAMPTON, VIRGINIA

Prepared for
National Aeronautics and Space Administration
Lewis Research Center
Under Grant NSG-3230

for
U.S. DEPARTMENT OF ENERGY
Conservation and Renewable Energy
Office of Vehicle and Engine R&D

NOTICE

This report was prepared to document work sponsored by the United States Government. Neither the United States nor its agent, the United States Department of Energy, nor any Federal employees, nor any of their contractors, subcontractors or their employees, makes any warranty, express or implied, or assumes any legal liability or responsibility for the accuracy, completeness, or usefulness of any information, apparatus, product or process disclosed, or represents that its use would not infringe privately owned rights

DOE/NASA/3230-1
NASA CR-165324

Transient Catalytic Combustor Model

James S. T'ien
Case Western Reserve University
Cleveland, Ohio

May 1981

Prepared for
National Aeronautics and Space Administration
Lewis Research Center
Cleveland, Ohio 44135
Under Grant NSG-3230

for
U.S. DEPARTMENT OF ENERGY
Conservation and Renewable Energy
Office of Vehicle and Engine R&D
Washington, D.C. 20545
Under Interagency Agreement DE-AI01-77CS51040

N82-13507 #

ACKNOWLEDGEMENT

This project is supported by the Department of Energy under NASA Grant NSG-3230 administered by NASA Lewis Research Center.

The author wishes to express his sincere thanks to Dr. David N. Anderson for helpful advice and his review of the manuscript.

TABLE OF CONTENTS

	PAGE
ABSTRACT	1
INTRODUCTION	2
Chapter I. Transient Catalytic Combustor Model	4
I.1 Nonsteady Combustion Model	4
Consideration of Time Scales	4
Quasisteady Gas Phase	5
Unsteady Solid with Thin-wall Substrate	9
Initial and Boundary Conditions	11
Numerical Solution Procedure	12
I.2 Computed Results	13
Steady State	13
Transient Response	19
Chapter II. Steady-State Computation and Comparison with Experiments	29
II.1 Three-step Semi-global Gas-phase Chemical Reactions	29
II.2 Computed Results	34
Effects of Catalytic Bed Length, Downstream Reaction Distance, Reference Velocity and Adiabatic Flame Temperature	36
Effect of Inlet Temperature and Pressure	43
SUMMARY	47
REFERENCE	49
NOMENCLATURE	51
Appendix I Listing of Computer Programmes for Chapter I.	55
Appendix II Listing of Computer Programmes for Chapter II.	72

ABSTRACT

A lean combustion model for monolithic catalytic combustors is given. The model, consisting of several semi-global chemical reaction steps in the gas phase and on the surface, is capable of analyzing CO and THC emissions and combustor efficiency in both steady and unsteady states.

In the steady-state model computation presented, the influence of operating and design parameters on the minimum combustor length is studied. Special attention is given to the effect of after-bed gas phase reaction space. Comparison with experimental data by Anderson indicates good agreement in the range of parameters covered.

In the transient analysis, a quasisteady gas phase and a thermally-thin substrate are assumed. The combustor response delay is due to the substrate thermal inertia. Fast response is found to be favored by thin substrate, short catalytic bed length, high combustor inlet and final temperatures and, in most cases, small gas channel diameters. The calculated gas and substrate temperature time history at different axial positions provide an understanding of how the catalytic combustor responds to an upstream condition change. The computed results also suggest that the gas residence times in the catalytic bed and in the after-bed space are correlatable with the nondimensional combustor response time. When fast transient responses are required, both steady and unsteady studies have to be made to achieve a meaningful compromising design.

INTRODUCTION

The operation and the design of catalytic combustors are limited on one end by the high temperature that the catalysts can tolerate and on the other end (low temperature) by the acceptable emission levels of CO and unburnt hydrocarbons. The aim of the combustion engineer is to design a compact and durable combustor capable of efficient and clean combustion. Catalytic combustor modeling can contribute to this objective by providing more understanding to the detail processes occurring in the reactor and to serve as a design guidance for minimizing the numbers of experimental tests needed.

There are several steady-state catalytic combustor models in existence (Ablow and Wise, 1979, Cerkanowicz, et al, 1977, Kelley et al, 1977, Kendall et al, 1979) and they show a high degree of success in describing the events occurring in the combustor. In particular, the model by Kelley et al (1977) containing detailed gas phase chemistry for methane/air reactions can predict pollutant emissions. Detailed kinetics, unfortunately, are not yet available for most other practical fuels. Since emission characteristics are important considerations for catalytic combustor design, in the absence of more detailed information, models consisting of several key semi-global chemical steps seem appropriate.

In addition to the emission characteristics, the transient behavior of catalytic combustors is expected to be different from that of a conventional gas turbine burner, due to the large thermal inertia of the substrate. Non-steady operations are obviously important to transportation engines since their power levels have to be changed frequently. Transients may also be a concern with stationary gas turbine applications, since the

ignition/shutdown operation can produce excessive thermal stress or thermal shock if the combustor is not designed or operated properly and the substrate can fail as a result (DeCorso and Carl, 1979).

Typical questions concerning transient operations include the combustor response time, the type of response, the unsteady substrate temperature history and the resultant thermal stress distribution. At the present time, both experiment and theory on transient catalytic combustion are lacking. A model is presented here attempting to analyze the problem theoretically. In Chapter I of this report, the transient combustion model will be formulated and numerical solution will be presented as a parametric study. Since the transient computer code can also yield steady-state results, in Chapter II, a detailed computation of steady states is given and a comparison with Anderson's data is made. As far as the combustion models are concerned, the one in Chapter II has a three-step global gas-phase chemical reaction vs. a two-step one in Chapter II. The reason for using the three-step scheme is discussed in the beginning of Chapter II.

I.1 Nonsteady Combustion Model

Consideration of Time Scales

For a monolithic catalytic combustor with uniform cell distribution in the plane normal to the approaching flow direction, if the combustor wall is well insulated, then the study of the whole reactor can be reduced to the consideration of a single cell unit. Referring to Fig. I.1, each cell unit consists of an open gas channel, the associated substrate volume and an after-bed gas reaction space.

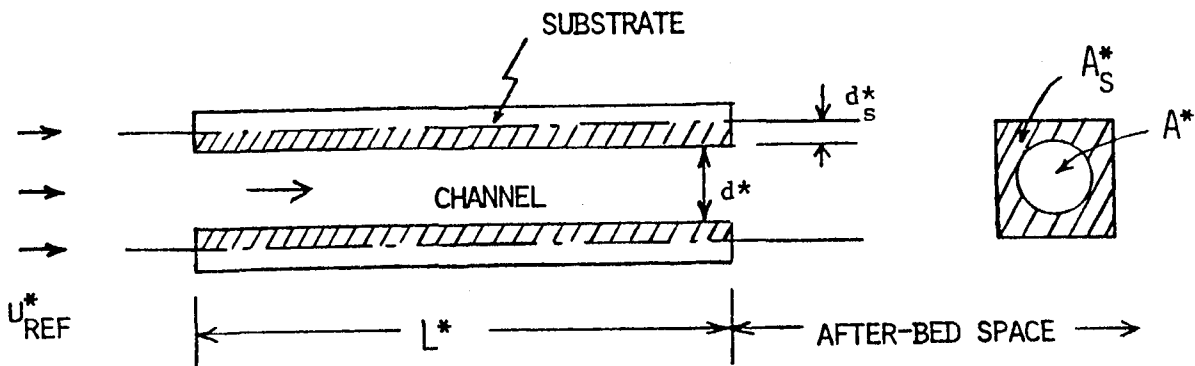


Figure I.1 Schematic Drawing of One Cell Unit

Considering first the steady-state combustion, the relevant time scales are the gas residence time in the reactor, the heat and mass transfer time between the gas and the solid surface inside the channel and the gas-phase and surface reaction times. When a transient is caused by an upstream parameter variation, then the new time scales involved include the input characteristic time, the time for the temperature wave to reach the central plane of the substrate and the time for heating-up (or cooling-down) the substrate.

Table I defines these characteristic times and their estimated magnitudes. It should be noted that some of the time scales vary along the channel of the reactor bed. For example, the heat/mass transfer time and the substrate heat-up time are shorter at the flow entrance region than those for far downstream, and the ones used in Table I are those based on fully-developed flow profiles. However, the estimation from Table I does serve the purpose of order-of-magnitude comparison. From this table we see that the longest time is the solid heat-up time, being of the order of seconds. If the time scale we are interested in is much greater than the gas residence time (~15 msec), then the gas phase processes (including heat/mass transfer and chemical reactions) can be regarded as in a quasi-steady state. If furthermore the substrate half-thickness is smaller than about .2 mm, then the substrate temperature distribution in the direction normal to the channel axis can be regarded as uniform at any given time. In this limiting case then, a "quasi-steady-gas-phase and thermally-thin-substrate" model is applicable with the only transient process being the substrate heating-up or cooling-down. In the following section, this model will be described in mathematical form.

Quasisteady Gas Phase

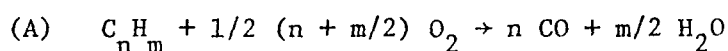
Quasisteady gas phase implies that the differential equations for the

Table I.1 Estimate of Transient Time Scales in Catalytic Monolith Combustor

Time	Definition	Estimated Magnitude
Gas residence time in reactor bed	$(L^*/u_{ref}^*) (A^*/A_T^*)$	1 - 15 msec
Gas residence time in after-bed space	L_{as}^*/u_{ref}^*	0 - 15 msec
Heat/mass transfer time between gas and solid surface in channel	$\frac{1}{Nu_{\infty}} \frac{1}{\pi} \frac{d_s^{*2}}{4\alpha^*(0,0)}$.5 - 7.5 msec for $d_s^* \leq 3.6$ mm
Chemical reaction times (gas-phase and heterogeneous)		Same order of magnitude as gas residence times
Time for temperature wave to reach the substrate center plane	$\frac{d_s^{*2}}{\alpha_s^*}$	0.5 - 25 msec for $d_s^* \leq .2$ mm
Substrate heat-up time	$\frac{1}{Nu_{\infty}} \frac{1}{\pi} \frac{A_s^* \rho_s^* C_s^*}{k^*(0,0)}$	0.5 sec - 20 sec
Transient input time		variable, specified

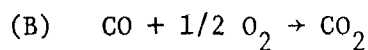
gas-phase processes are the same as those for the steady state. Only the boundary conditions on the solid surface are different. There are several steady-state catalytic combustor models in existence [Cerkanowicz et al, 1977, Kelly et al, 1977, 1979] and they show a high degree of success in describing the events occurring in the combustor. In particular, the model by Kelley et al (1977) containing detailed chemistry for methane/air reactions can predict pollutant emissions. Detailed kinetics, unfortunately, are not yet available for most other practical fuels. Since emission characteristics are important considerations for catalytic combustor design, in the absence of more detailed information, a model consisting of several key semi-global chemical steps is proposed.

For fuel-lean catalytic combustion using nitrogen-free hydrocarbon fuels, the NO_x emission is negligible because of low flame temperatures. The only pollutants needed to be considered are unburnt hydrocarbons (UHC) and carbon monoxide (CO). For this reason, the two semi-global chemical reactions used in the gas phase are:



$$\frac{d[\text{C}_n\text{H}_m]}{dt^*} = -C_1^* p^{*\alpha_1} [\text{C}_n\text{H}_m]^{\alpha_2} [\text{O}_2]^{\alpha_3} T^{*\alpha_4} \exp(-E_1^*/RT^*)$$

(1)



$$\frac{d[\text{CO}]}{dt^*} = -C_2^* p^{*\beta_1} [\text{CO}]^{\beta_2} [\text{O}_2]^{\beta_3} [\text{H}_2\text{O}]^{\beta_5} T^{*\beta_4} \exp(-E_2^*/RT^*)$$

(2)

In describing the flow in the reactor channel, we follow previous investigators in using the plug flow approximation. For transient cases, in general, the fluid properties are functions of x , the distance along the channel axis and t , the time. For example, density of the gas will be

expressed as $\rho(x,t)$. The nondimensional forms of these equations are summarized in the following (superscript * denotes dimensional quantity and without * denotes nondimensional quantities).

$$\text{Continuity: } \rho u = \hat{\rho}(0,t) u(0,t) \quad (3)$$

$$\text{Momentum: } p = p(0,t) \quad (4)$$

$$\begin{aligned} \text{Energy: } \quad \rho u \frac{\partial T}{\partial x} + J_H(T - T_S) &= q_1 Y_{HC}(0,0) w_1 \\ &+ q_2 Y_{HC}(0,0) w_2 \end{aligned} \quad (5)$$

Species:

Hydrocarbon:

$$\rho u \frac{\partial y_{HC}}{\partial x} + J_{D_1} (y_{HC} - y_{HC,S}) = -w_1 \quad (6)$$

Carbon monoxide:

$$\rho u \frac{\partial y_{CO}}{\partial x} + J_{D_2} (y_{CO} - y_{CO,S}) = w_1 C_n - w_2 \quad (7)$$

Oxygen:

$$y_{O_2} = 1 - \phi(1 - y_{HC}) + \frac{1}{2} y_{CO} \left(\frac{Y_{HC}(0,0) W_{O_2}}{Y_{O_2}(0,0) W_{CO}} \right) \quad (8)$$

$$\text{Equation of state: } p = \rho T \quad (9)$$

The reaction rates are given by

$$w_1 = B_1 p^{\alpha_1} \rho^{(\alpha_2 + \alpha_3)} T^{\alpha_4} y_{HC}^{\alpha_2} y_{O_2}^{\alpha_3} e^{-(E_1/T)} \quad (10)$$

$$w_2 = B_2 p^{\beta_1} \rho^{(\beta_2 + \beta_3 + \beta_5)} T^{\beta_4} y_{CO}^{\beta_2} y_{O_2}^{\beta_3} Y_{H_2O}^{\beta_5} e^{-(E_2/T)} \quad (11)$$

$$\text{and } Y_{H_2O}(x,t) = \frac{m}{2} \frac{W_{H_2O}}{W_{HC}} Y_{HC}(0,0) \left[y_{HC}(0,t) - y_{HC}(x,t) \right] \quad (12)$$

The definition of B_1 and B_2 can be found in the nomenclature.

In deriving Eqns (5-8), heat conduction and mass diffusion in the axial direction are neglected because the Peclet number based on typical gas velocity (>10 M/sec) is much greater than unity [Ablow and Wise, 1979]. The dimensionless lateral heat and mass transfer coefficients J_H and J_{Di} , in Eqns (5-7) are derived from Nusselt number calculation in entrance flow in a tube of constant surface temperature [Kays, 1966]. Following Kelly et al (1977), a modification is made at the entrance point based on local stagnation flow estimation. The use of entrance flow transport properties, rather than fully-developed constant values, make a great difference in the temperature and species distributions in the flow entrance region.

The above system of equations can also be applied to the after-bed space where only gas-phase reactions occur. This is done by putting J_H and J_{Di} equal to zero in Eqns (5-7) and by properly changing the mass flux per unit area in Eq (3) due to area change.

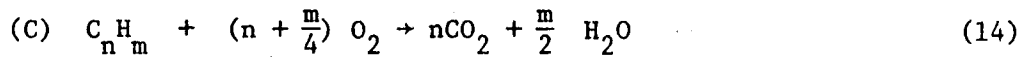
Unsteady Solid with Thin-Wall Substrate

When the substrate wall is thermally thin, the solid temperature can be regarded as a function of axial distance and time only, i.e., $T_s(x,t)$. The energy balance of the solid, including the solid surface, results in the following equation:

$$A_s^* \rho_s^* C_s^* \frac{\partial T_s^*}{\partial t^*} - h_T^* S^* (T^* - T_s^*) = S^* [q_3^* J_3^* + q_4^* J_4^*] \quad (13)$$

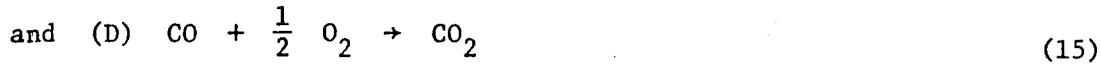
In Eq (13) the heat conduction in the axial direction in the solid is neglected in comparison with the heat transfer rate between the gas and solid across the gas channel.

Two semi-global catalytic surface reactions are assumed. They are



with the corresponding surface reaction rate J_3^* given by

$$J_3^* = C_3^* [C_n H_m]_s e^{-E_3^*/RT_s^*}$$



with $J_4^* = C_4^* [CO]_s e^{-E_4^*/RT_s^*}$

In surface reaction (C), the hydrocarbon is oxidized to form CO_2 and H_2O , not CO such as in gas-phase reaction (A). This is based on the present available experimental evidence in oxygen-rich systems, only CO_2 , not CO , is found on or close to the catalytic surface [Schwartz et al, 1971, Anderson, 1976 and Marteney, 1979].

Eq (13) is non dimensionalized by first defining a proper reference time scale τ^* .

$$\tau^* \equiv \frac{1}{Nu_\infty} \frac{1}{\pi} \frac{A_s^* \rho_s^* C_s^*}{k^*(0,0)} \quad (16)$$

and $t \equiv t^*/\tau^*$

$$r_{nk} \equiv \frac{Nu_x}{Nu_\infty} \frac{k^*}{k^*(0,0)} \quad (17)$$

Eq (13) becomes

$$\begin{aligned} \frac{\partial T_s}{\partial t} - r_{nk} (T - T_s) = & B_3 Y_{HC}(0,0) q_3 \rho y_{HC,s} \exp(-E_3/T_s) \\ & + B_4 Y_{HC}(0,0) q_4 \rho y_{CO,s} \exp(-E_4/T_s) \end{aligned} \quad (18)$$

Neglecting transient accumulation on the surface, the surface hydrocarbon and carbon monoxide are given by

$$r_{nk} (y_{HC} - y_{HC,s}) = \frac{1}{(L_{e1})^{2/3}} B_3 \rho y_{HC,s} \exp(-E_3/T_s) \quad (19)$$

$$r_{nk} (y_{CO} - y_{CO,s}) = \frac{1}{(L_{e2})^{2/3}} B_4 \rho y_{CO,s} \exp(-E_4/T_s) \quad (20)$$

Initial and Boundary Conditions

The system of equations (3-12, 18-20) needs initial and boundary conditions. Initial conditions (at $t = 0$) are required for T_s , $(y_{HC})_s$, $(y_{CO})_s$ as a function of x and upstream boundary conditions (at $x = 0$) should be specified for y_{HC} , y_{CO} , y_{O_2} , T , p and u as a function of time. These conditions depend on the types of transient input which can vary with engine designs and mode of operations. In the present paper, a simple start-up transient is investigated, i.e. catalytic combustor response to a step-wise fuel injection.

The substrate temperature at time $t=0$ is specified. This temperature can be the result of external heating of the substrate, say, by a torch. The fuel and air are then supplied at upstream. The model is intended to describe the events from $t=0$ to the final steady state. Mathematically, the conditions used are

$$T_s(x,0) = \text{specified}$$

$$y_{\text{HC},s}(x,0) = 0$$

$$y_{\text{CO},s}(x,0) = 0$$

$$T(0,t) = 1$$

(21)

$$y_{\text{HC}}(0,t) = 1$$

$$y_{\text{CO}}(0,t) = 0$$

$$y_{\text{O}_2}(0,t) = 1$$

$$p(0,t) = 1$$

$$u(0,t) = 1$$

Numerical Solution Procedure

Although most dependent variables in this problem are function of both x and t which, in general, results in partial differential equations, the assumption of quasisteady gas phase and thermally thin substrate greatly simplifies the mathematical property of the system and results in a simpler solution procedure.

The gas-phase differential equations (5-7) have only first derivative in x with t as a parameter, the solid equation (18) has only derivative in t with x as a parameter; therefore, they can be integrated at each time (t) or position (x) as ordinary differential equations using Runge-Kutta method. The procedure is started by first integrating Eqns (5-7) forward in x from upstream to the end of combustor for T , y_{HC} , y_{CO} using the solid surface

quantities specified by the initial conditions, then Eq (18) is integrated for one time step (Δt) to find $T_g(x, \Delta t)$ and Eqns (19,20) are solved algebraically to find $y_{HC,s}(x, \Delta t)$ and $y_{CO,s}(x, \Delta t)$. These surface quantities are substituted back to Eqns (5-7) to start another cycle of integration. Steady-state and transient solutions are obtained using the same code. The computational time ranges from 10-50 seconds in a VAX-11 computer. The numerical scheme is an efficient one and it is suitable for parametric studies.

I.2 Computed Results

Steady State

Selected steady-state results will be presented first to facilitate the discussion on the transient response. Specifically, the relative importance of the catalytic bed length and the after-bed-gas-phase-reaction distance will be shown. In previous theoretical models, emphasis was placed on the combustion inside the catalytic bed only. The contribution of gas-phase reactions in the downstream space after the bed has been demonstrated in the experiments by T'ien and Anderson (1979) and Anderson (1980). Utilization of the pure gas-phase reactions in the downstream of the monolith to replace a portion of the catalytic bed will be shown to be crucial in reducing the catalytic combustor transient response time.

Table I.2 lists the values of chemical kinetic constants for reactions A to D used in this chapter. The hydrocarbon fuel chosen is propane. Semi-global kinetics for hydrocarbon and CO oxidation are from Edelman (1969) and Dryer and Glassman (1973) respectively, with the pre-exponential factors

Table I.2 Chemical Kinetic Constants for Chapter I

Reaction (A)	Reaction (B)	Reaction (C)	Reaction (D)
$C_1^* = 1.5 \times 10^5$	$C_2^* = 0.71 \times 10^{14}$	$C_3^* = 2.5 \times 10^3$	$C_4^* = 10^5$
$\alpha_1 = 0.3$	$\beta_1 = 0$	$E_3^* = 10$ (kcal/mole)	$E_4^* = 17.8$ (kcal/mole)
$\alpha_2 = 0.5$	$\beta_2 = 1$		
$\alpha_3 = 1$	$\beta_3 = 0.25$		
$\alpha_4 = 1$	$\beta_4 = 0$		
$E_1^* = 24$ (kcal/mole)	$\beta_5 = 0.5$ $E_2^* = 40$ (kcal/mole)		

adjusted. The activation energies for reactions C and D are obtained from the data of Marteney (1979) and Kuo and Morgan (1971) respectively with adjusted pre-exponential factors. It should be noted that the surface reaction rates contain information on catalyst type and loading density as well as the washcoat properties.

The design parameters considered are d^* , channel hydraulic diameter, A^*/A_T^* , the percentage of open area (or equivalently, A^*/A_S^* , the ratio of open-to-close areas), L^* , the catalytic bed length and L_{as}^* , after-bed gas-phase reaction length. The minimum catalytic combustor length required to reach the emission goal in steady-state operations is denoted using the subscript EG. The emission goal is chosen to be 1.64 g/kg of fuel for UHC and 13.6 g/kg of fuel for CO [Anderson, 1977]. The operating parameters include p^* , the pressure, T_{in}^* , combustor inlet temperature, T_{af}^* , adiabatic flame temperature (or equivalently the fuel/air equivalence ratio ϕ) and U_{ref}^* , the reference velocity of the approach gas upstream of the reactor bed.

Fig. I.2 gives the profiles for one sample calculation. In this case, the propane fuel is oxidized quickly on the catalyst surface upon entering into the reactor channel and resulting in a high surface temperature, the gas temperature is raised by heat transfer from the substrate, gas-phase oxidation of propane is accelerated to form CO, and CO, in turn, is oxidized by both gas-phase and surface reactions to CO_2 . Actually, two cases are shown in Fig.I.2. In one case, the reactor bed length is 4 cm, in the other, 8 cm. When the bed length is cut short at 4 cm, the surface oxidation reactions for the hydrocarbon fuel and CO stop there. This results in a higher CO concentration as shown by the dotted curve. The hydrocarbon curve

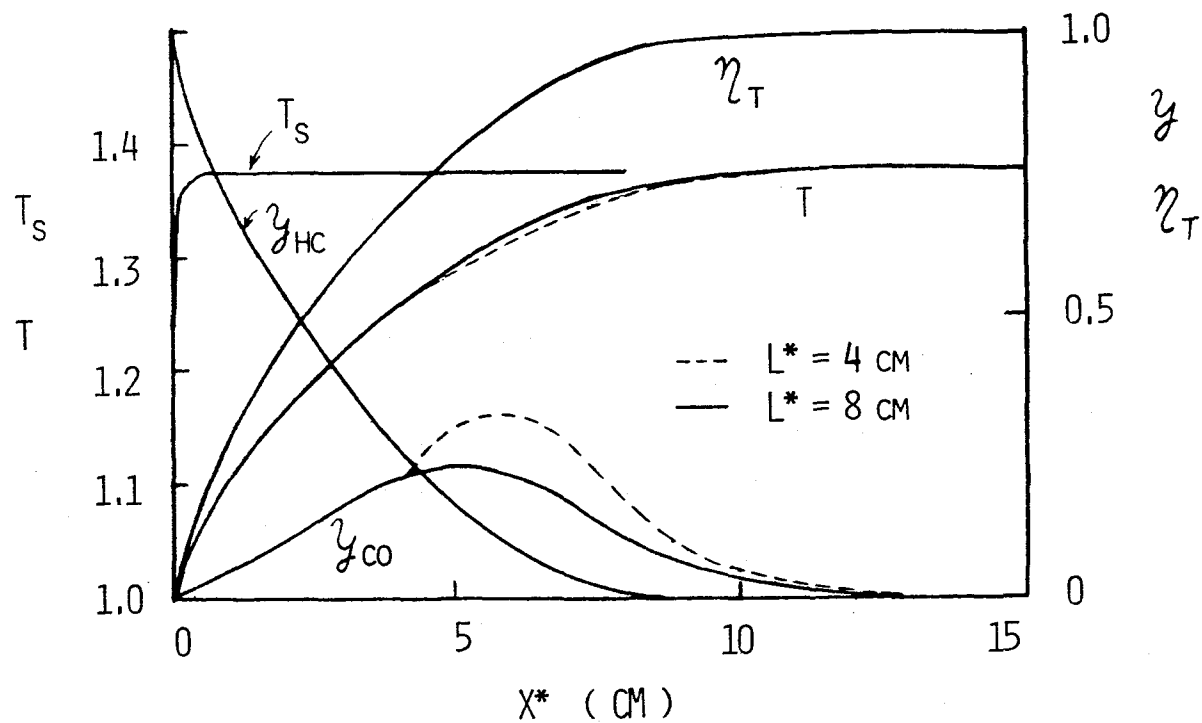


Figure I.2 Detailed steady-state profiles showing the effect of catalytic bed length. Operating conditions: $p^* = 3 \text{ atm}$, $T_{in}^* = 1000^\circ\text{K}$, $u_{ref}^* = 10 \text{ m/s}$, $\phi = 0.15$, $d^* = 1.8 \text{ mm}$ and $A^*/A_T^* = .667$.

also shows a difference after 4 cm but the difference is too small to be shown clearly in this figure. The gas temperature is also lower in a portion of the combustor for the 4 cm case.

Fig. I.3 gives the combustor residence time required to reach the emission goal vs. the residence time in the catalytic bed. The "catalytic bed residence time", t_b^* , is defined by $L^*A^*/U_{ref}^* A_T^*$, where U_{ref}^* is the gas velocity upstream of the bed and the gas velocity inside the catalytic channel at the channel entrance is $U_{ref}^* A_T^*/A^*$, due to the area change. To be exact, the gas residence time in the bed should be $\int_0^{L^*} 1/U^* dx^*$ since the gas velocity in the channel, U^* , is changing continuously downstream due to the heat release. However, since $U^*(x)$ is not known until the solution is achieved, the catalytic bed residence time, t_b^* , as defined in Fig. I.3 is a good reference quantity and it is with this understanding when we use the terms of "bed residence time" and "combustor residence time".

Referring to the curve and the calculated points corresponding to $T_{in}^* = 1000$ K in Fig. I.3 we see that the residence times provide an excellent correlation for different values of U_{ref}^* , L^* , A^*/A_T^* and the required L_{as}^* to reach emission goals. As the catalytic bed residence time, t_b^* , increases, the total combustor residence time required to reach emission goals, t_{EG}^* , first decreases sharply and then levels off. The two other curves in Fig. I.3 give the effects of different combustor inlet temperatures. Higher inlet temperature required lower combustor residence time to reach emission goals for a fixed catalytic bed residence time. At 1200 K inlet temperature, no catalytic element is needed; emission goals can be reached in an acceptable gas residence time for a plug flow combustor without flame stabilizer ($t_b^* = 0$ and $T_{EG}^* = 14$ seconds). This has been verified by the recent

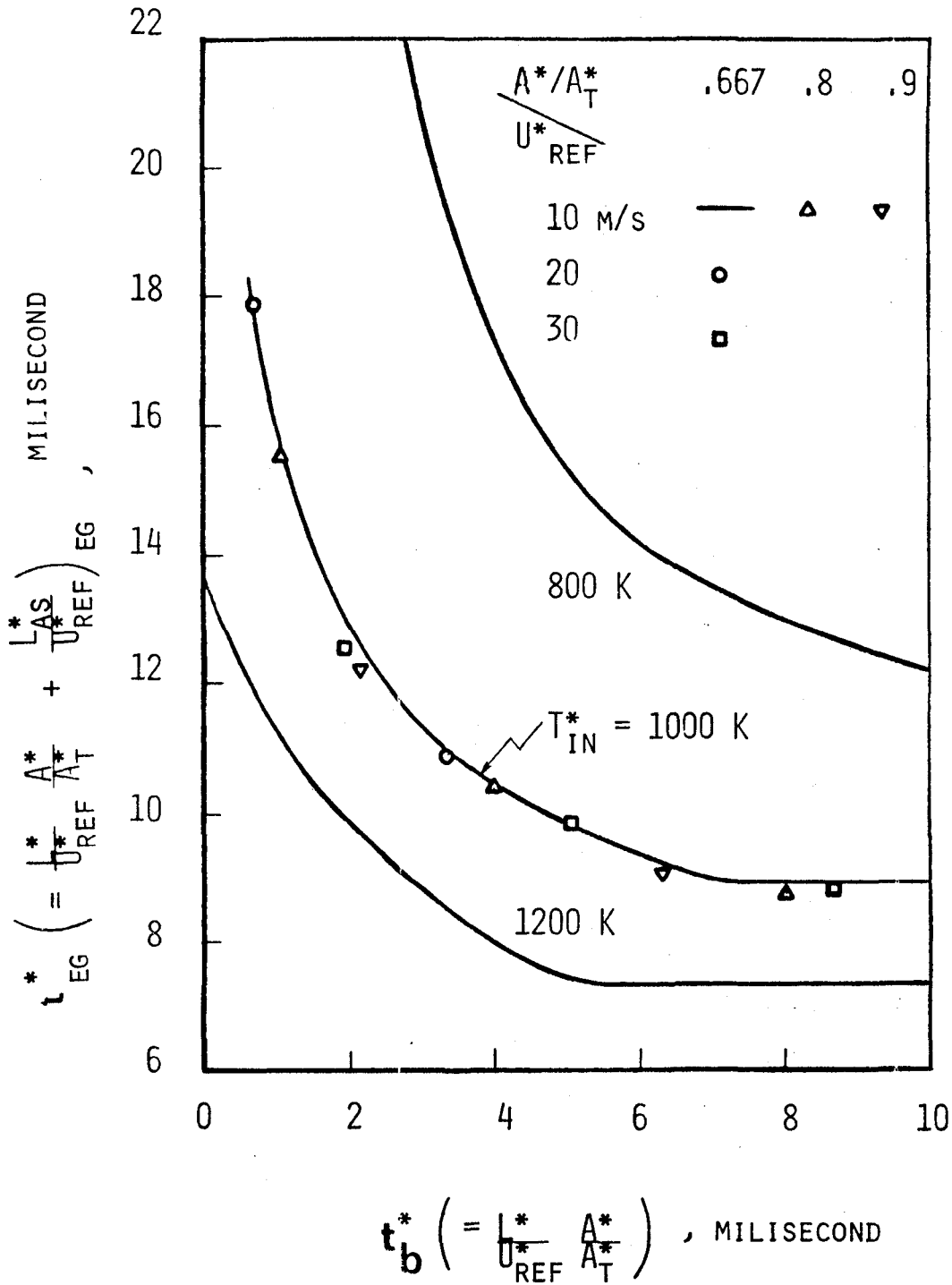


Fig. I.3 Minimum total combustor gas residence time for reaching emission goals (t_{EG}^*) vs. reactor bed residence time (t_b^*) as a function of combustor inlet temperature in steady-state operation. $p^* = 3$ atm, $d^* = 1.8$ mm and $T_{af}^* = 1370$ K.

experimental results of Anderson (1980b). Anderson's study also suggested the correlation using gas residence times (1980a).

Transient Response

One of the major concerns of the catalytic combustor application to transportation gas turbine engines is that the response time might be long. The computed transient results to be presented are combustor response to a stepwise increase of fuel flow rate (zero to a fixed value). Its purpose is to guide the search for "fast-response" catalytic combustor designs.

Some indication of the order of magnitude of the response time can be obtained from the definition of the characteristic time τ^* as defined in Eq (16). Small τ^* requires small thermal inertia, $A_s^* \rho_s C_s^*$. If the substrate density and heat capacity are fixed, small τ^* can be achieved with small solid crosssectional area A_s^* , see Fig. I.1 for definition of A_s^* . It should be noted that there are other parameters such as catalytic bed length and channel diameter which will influence the response time and they are not contained in τ^* . This will be discussed later as we see the computed results.

The combustion efficiency at the end of the combustor will be used to characterize the combustor response time. There are two ways to define the combustion efficiency. One is the so-called "carbon-balanced" efficiency, η_{CB} [Anderson, 1975], where the combustion inefficiency is measured by the emission levels of CO and UHC and the energy carried away by them. The other efficiency is the ordinary one defined by the enthalpy rise across the combustor divided by the chemical energy available. If the gas specific heat is approximated as a constant, this efficiency, η_T , is given by $(T^* - T_{in}^*) / (T_{af}^* - T_{in}^*)$ where T^* is measured at the same location as the efficiency. For a perfectly insulated catalytic combustor in steady state,

η_{CB} and η_T are the same. However, the two are different in transient operations when there is a thermal lag in the substrate.

For the following transient calculation, the initial surface temperature condition is given by $T_s(x,0) = 1$, see Eq (21). For 1000°K inlet temperature, two bed lengths, 4 cm and 8 cm, are chosen for the transient calculation and efficiency is evaluated at their individual minimum combustor lengths according to Fig.I.3. Fig.I.4 shows the combustion efficiencies as a function of non-dimensional time. Looking at the curves for η_T (efficiency based on temperatures), the shorter bed (4 cm) combustor has a faster response than that of the longer bed (8 cm). If we take the time for η_T to reach 80% as an indication of characteristic response time, for the 4 cm bed, $t_{ch} = 1.5$ and for the 8 cm bed, $t_{ch} = 2.5$; namely, the response time of 4 cm bed combustor is only 60% of that of the 8 cm bed combustor. From the consideration of steady-state operation alone, one would choose the 8 cm catalytic bed since, as can be deduced from Fig.I.3, this produces the shortest required combustor length (11 cm). However, combining transient and steady-state considerations, the 4 cm bed combustor may be a better choice as its response time is 60% of that of the 8 cm bed, with the total combustor length only slightly longer.

To understand why longer reactor bed results in a longer response time, surface and gas temperature distributions are plotted in Fig. I.5 as a function of time. From the substrate temperature distribution we see that during start-up transient, the solid temperature is higher in the flow entrance region as a result of higher mass transport and surface reaction rates. Comparing the solid and gas temperature histories for the case when catalytic bed length is 8 cm, we see that at $t = 0.5$, the solid is

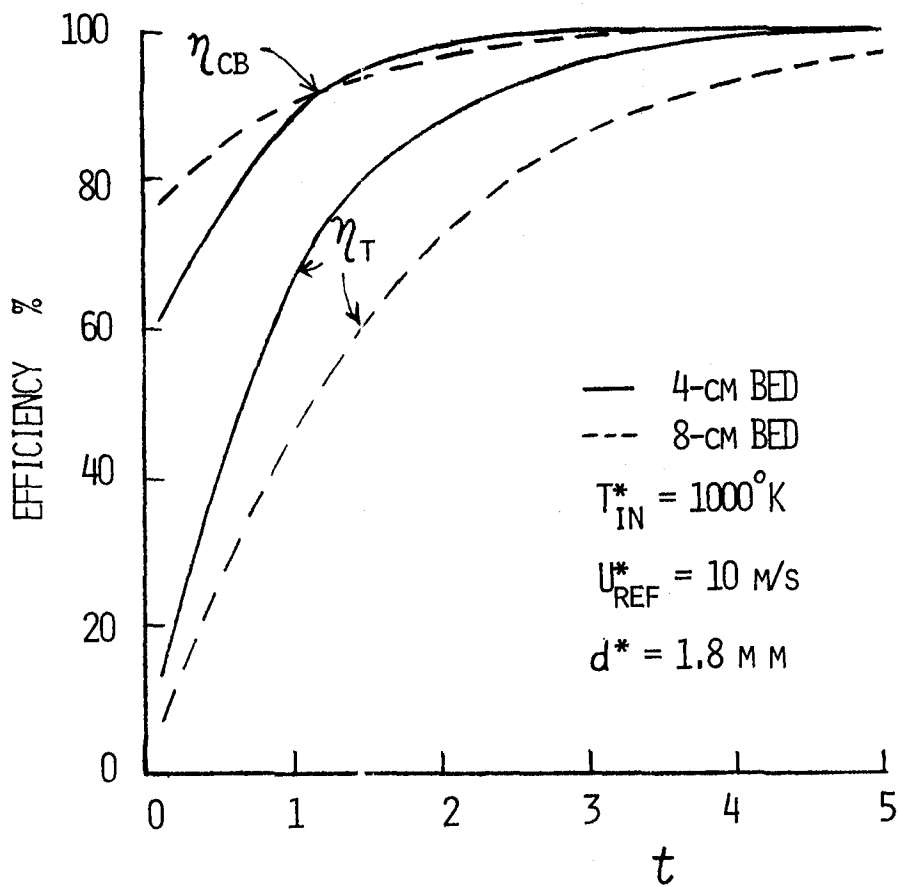


Fig. I.4 Combustion efficiencies as a function of time during start-up transient. $p^* = 3 \text{ atm}$, $\phi = 0.15$ and $A^*/A_T^* = .667$.

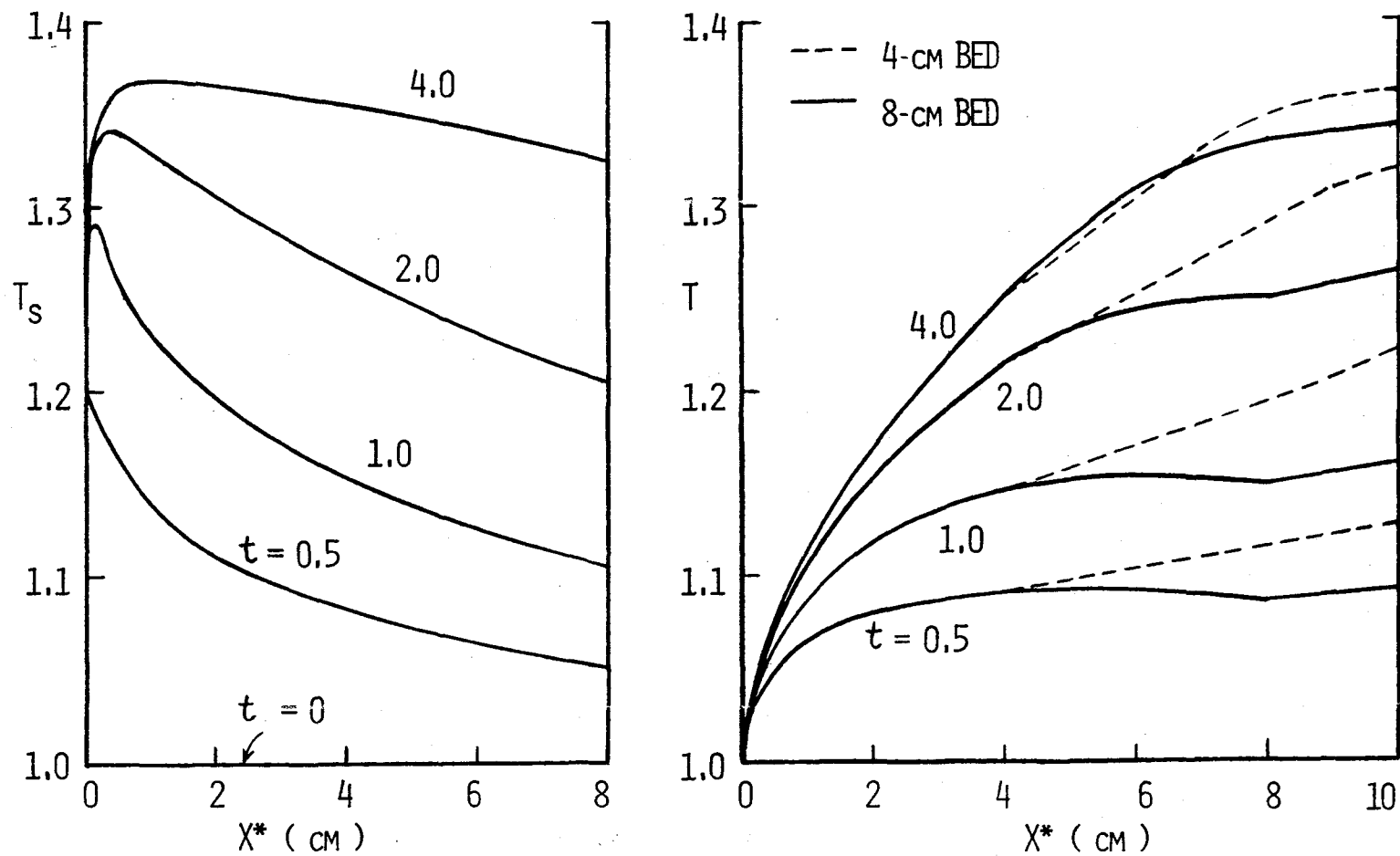


Fig.I.5 Gas and substrate temperature history during transient start-up for two bed lengths. Same operating and design parameters as those in Fig.I.4.

transferring heat to the gas in the upstream region in the bed. At $x^* = 3.5$ cm, the gas temperature becomes higher than the substrate temperature, heat is then transferred from the gas to the solid in the down-stream portion of the reactor channel. If the heat loss rate is greater than heat generation rate due to gas phase reactions, then the gas temperature will drop as shown in Fig.I.5. If we cut the reactor bed short at 4 cm, a portion of this heat loss can be eliminated and the downstream gas temperature ($x^* > 4$ cm) will be higher as indicated by the dotted curves in Fig.I.5. This explains why a shorter reactor bed can have a faster response.

More computation of the response time dependence on the catalytic bed length, gas velocity and combustor inlet temperature is shown in Fig. I.6. As will be shown later, the nondimensional transient response also correlates well with the gas residence times in the reactor bed and the after-bed space. Therefore the results will be presented using residence times rather than length and velocity. In Fig.I.6, the adiabatic flame temperature, pressure, channel diameter, open area fraction and L^*/U_{ref}^* are held constant. The solid line in Fig.I.6 gives the response time if the reactor-bed-gas-residence time is the minimum to reach emission goals in steady-state operations. When the combustor inlet temperature is increased, the minimum required reactor-bed-residence time is decreased and the combustor response time is shortened drastically. If a more conservative design is used, i.e. longer bed residence time than is required, the combustor response time is increased for a fixed inlet temperature. The increase is very slight in the beginning when the bed residence time is close to the optimum value but becomes larger as the bed residence time increase further. This implies that a conservative

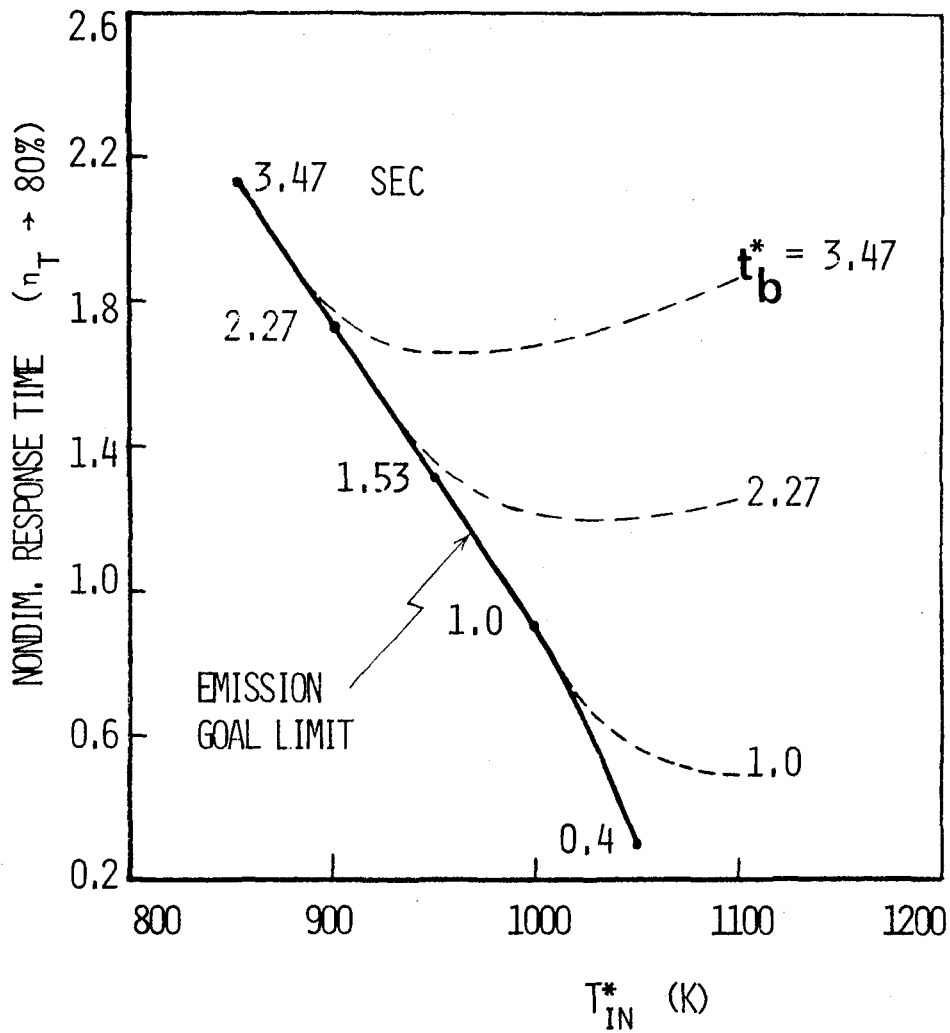


Fig.I.6 Nondimensional response time (η_T goes to 80%) as a function of combustor inlet temperature and reactor bed residence time. $L^*/U^*_{ref} = 15$ msec, $T^*_{af} = 1370$ K, $A^*/A^*_T = .667$, $d^* = 1.8$ mm and $p^* = 3$ atm.

design with reactor bed length somewhat longer than that of the optimal one will not greatly increase the combustor response time.

Fig.I.7 gives the nondimensional response time as a function of channel hydraulic diameter and flame temperature. For all the calculations in Fig.I.7 the residence time in the catalytic bed, t_b^* , is held constant at 1 millisecond and the residence time in the after-bed space, t_{as}^* , is 13.5 milliseconds. The computation for 1370 K and 1590 K includes different combinations of L^* , L_{as}^* , U_{ref}^* and A^*/A_s^* and it can be seen from Fig.I.7 that the nondimensional response time correlates well with the residence times. *It can, therefore, be concluded that the primary influence of the catalytic bed and after-bed lengths, the approaching gas velocity and the open area percentage is contained in the gas residence times in the catalytic bed and in the after-bed space for both steady and transient operations.*

Fig. I.7 also shows that for a given flame temperature, the nondimensional response time increases with decreasing channel diameter d^* . This, however, does not necessarily mean that the dimensional response time increases with decreasing d^* . If the open area percentage (or equivalently A^*/A_s^*) is fixed, decreasing d^* decreases A_s^* which is used in the reference time scale as defined in Eq (16) and the dimensional response time may actually decrease. Table I.3 gives selected dimensional response times for ceramic and Kanthal metal alloy substrates using the computed results from Fig.I.7. It can be seen that in general the dimensional response time decreases with decreasing channel diameter but the amount of decrease vanishes when the channel diameter becomes too small. In special cases such as the 1590 K flame temperature case, the response time actually reaches a minimum and increases with further diameter decrease.

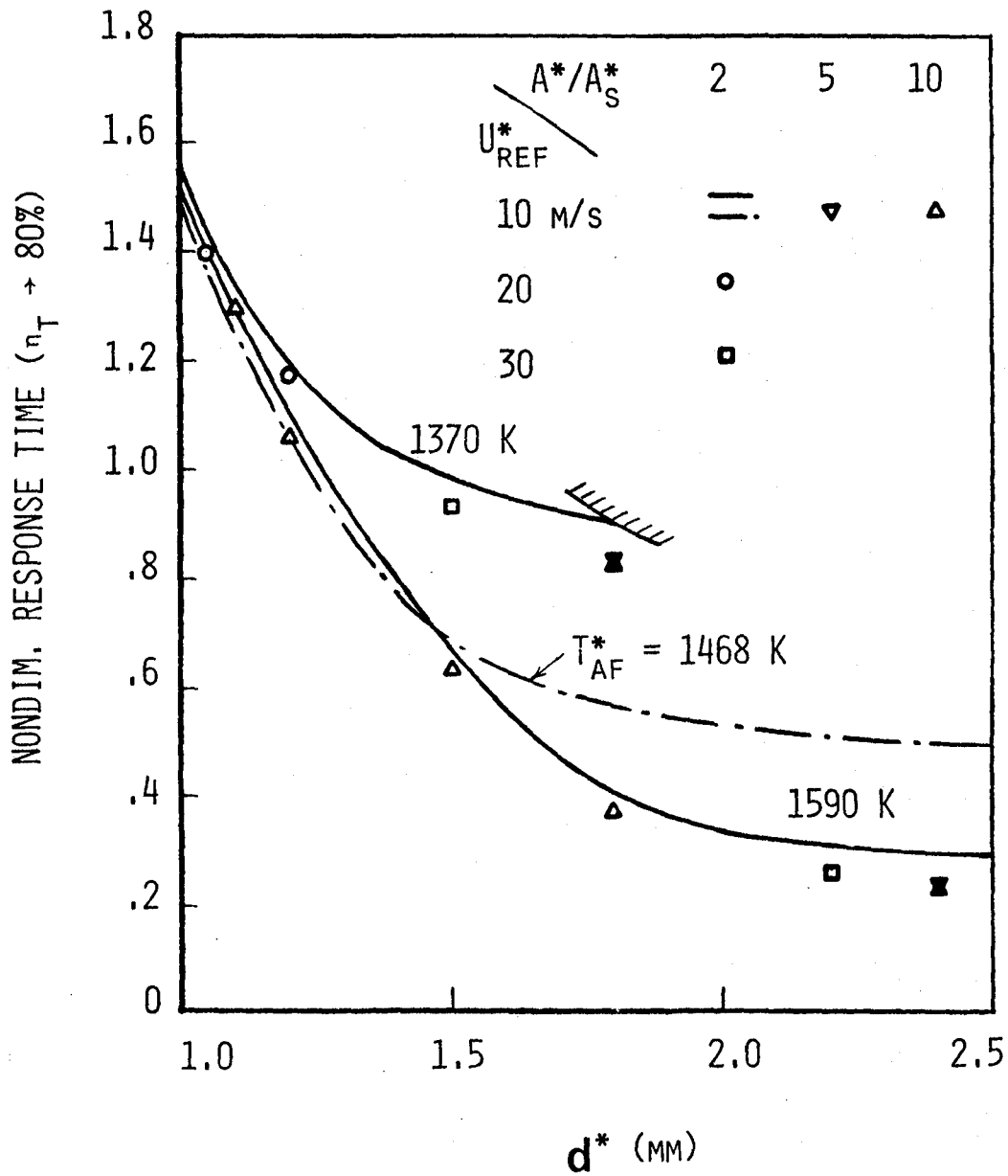


Fig. I.7 Computed nondimensional catalytic combustor response time correlation with gas residence times for various channel diameters and flame temperatures. $p^* = 3 \text{ atm}$, $t_b^* = 1 \text{ msec}$, $t_{as}^* = 13.5 \text{ msec}$, $T_{in}^* = 1000 \text{ K}$.

Table I.3 Computed Catalytic Combustor Response Time Using Ceramic
and Kanthal Metal Substrates.

$t_b^* = 1$ msec, $t_{as}^* = 13.5$ msec, $p^* = 3$ atm, $T_{in}^* = 1000$ K

T_{af}^* (K)	A^*/A_s^*	d^* (mm)	t_r^* (sec) ceramic	t_r^* (sec) Kanthal alloy
1370	10	1.8	.848	1.52
1370	10	1.0	.451	.807
1468	10	2.5	.909	1.63
1468	10	1.8	.533	.956
1468	10	1.0	.454	.813
1590	10	2.5	.527	.944
1590	10	1.8	.377	.675
1590	10	1.0	.448	.802
1590	5	1.8	.754	1.35
1590	2	1.8	1.88	3.37

If the gas residence times and channel diameter are held constant, varying the open area percentage (or A^*/A_s^*) changes the dimensional response time by a factor of A_s^*/A^* . This is the direct consequence of the correlation between nondimensional response time and residence times as just discussed. Large open area percentage (or thin substrate), therefore, favors fast response.

Fig I.7 indicates higher flame temperature shortens the response time for large diameter channel but flame temperature makes little difference in response time for very small diameter channels as all curves converge.

II.1 Three-step Semi-global gas-phase Chemical Reactions

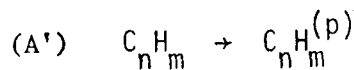
Gas phase reaction studies between hydrocarbons and air in lean mixtures have shown (Dryer and Glassman, 1978) that the hydrocarbon fuel first decomposes into a number of lower hydrocarbons with the simultaneous formation of some water vapor. The combination of these "pyrolysis" steps results in an almost isothermal region after which CO is formed and temperature begins to rise. The carbon monoxide is then oxidized and the reactions are completed. These kinetic studies are very useful for the development of semi-global kinetic schemes.

Two recent catalytic combustion models, by Bracco et al (1980) and T'ien (1980), have utilized the gas phase semi-global modeling concept. The study by T'ien was actually for transient response but a quasisteady gas phase was assumed. The gas phase reactions consist of two semi-global steps; the hydrocarbon reacts with oxygen to form CO and H₂O and CO then reacts with oxygen to form CO₂. On the surface, both hydrocarbon and CO react with oxygen to form CO₂ and or H₂O. The steady-state prediction of that model agrees qualitatively with the experimental trend of CO and hydrocarbon emissions, but a quantitative comparison has not been made. From a pure gas phase reaction point of view, two-step semi-global scheme predicts too high a level of CO in the initial pyrolysis region even though the CO peak level and the decay curve can be made to agree with the experimental data by kinetic parameter adjustment. This early CO appearance problem can be alleviated to a certain

extent by increasing the number of appropriate semi-global gas reaction steps. In the work by Bracco et al (1980), for example, a three-step reaction scheme was used for propane oxidation. Propane (C_3H_8) was assumed to form C_2H_4 first, C_2H_4 to CO next and then CO to CO_2 .

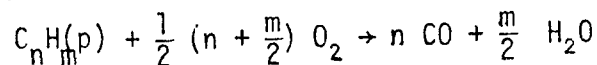
For most practical fuels, the pyrolysis intermediates are numerous, and a dominant intermediate species may or may not exist. Since in high inlet temperature operations ($T_{in}^* > 800^{\circ}K$), the catalytic combustor length required is limited by the emission level of CO, not hydrocarbons (Anderson, 1980a), it seems reasonable to develop a scheme which gives the correct CO characteristics without being tied down by the uncertain nature of the hydrocarbon intermediates.

In this chapter, the steady-state computation will be based on a three-step gas-phase kinetic scheme. The semi-global reactions are:

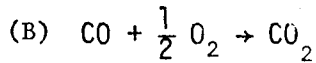


$$\frac{d[C_n H_m]}{d t^*} = - C_0^* p^{*\gamma_1} [C_n H_m]^{\gamma_2} T^{*\gamma_3} \exp(-E_0^*/RT^*) \quad (22)$$

(A'')



$$\frac{d[C_n H_m^{(p)}]}{d t^*} = - C_1^* p^{*\alpha_1} [C_n H_m^{(p)}]^{\alpha_2} [O_2]^{\alpha_3} T^{*\alpha_4} \exp(-E_1^*/RT^*) \quad (23)$$



$$\frac{d[\text{CO}]}{d t^*} = - C_2^* p^{*\beta} {}_1 [\text{CO}]^{\beta} {}_2 [\text{O}_2]^{\beta} {}_3 [\text{H}_2\text{O}]^{\beta} {}_5 T^{*\beta} {}_4 \times \exp(-E_2^*/RT^*)$$

(24)

In reaction (A'), Eq. (22), the original hydrocarbon fuel forms the "pyrolyzed hydrocarbon", $\text{C}_n\text{H}_m^{(P)}$, in an isothermal reaction. The "pyrolyzed hydrocarbon" then reacts with oxygen to form CO and H_2O in reaction (A''). In reaction (B), CO is oxidized to CO_2 . The introduction of reaction (A') serves to decrease the amount of early CO appearance as found using the two-step model. The identity of $\text{C}_n\text{H}_m^{(P)}$ is of no great consequence for the purpose of this modeling work, if the mass diffusion coefficient is properly evaluated. For convenience, in the present calculation we take $\text{C}_n\text{H}_m^{(P)}$ to have the same n and m as the original fuel.

Corresponding to the reactions given by Eqs. (22-24), the species equations are:

Original Hydrocarbon:

$$\rho u \frac{d y_{\text{HC}}}{dx} + J_{D_1} (y_{\text{HC}} - y_{\text{HC},s}) = - w_o \quad (25)$$

"pyrolyzed" Hydrocarbon:

$$\rho u \frac{d\gamma_{HC}^{(p)}}{dx} + J_{D1} (\gamma_{HC}^{(p)} - \gamma_{HC,s}^{(p)}) = w_0 - w_1 \quad (26)$$

Carbon monoxide:

$$\rho u \frac{d\gamma_{CO}}{dx} + J_{D2} (\gamma_{CO} - \gamma_{CO,s}) = w_1 C_n - w_2 \quad (27)$$

Oxygen:

$$\gamma_{O_2} = 1 - \phi (1 - \gamma_{THC}) + \frac{1}{2} \gamma_{CO} \left(\frac{\gamma_{HC}^{(o)} w_{O_2}}{\gamma_{O_2}^{(o)} w_{CO}} \right) \quad (28)$$

where

$$\gamma_{THC} = \gamma_{HC} + \gamma_{HC}^{(p)}$$

The reaction rates are given by

$$w_0 = B_0 \rho^{Y_1} T^{Y_2} \gamma_{HC}^{Y_3} \exp(-E_0/T) \quad (29)$$

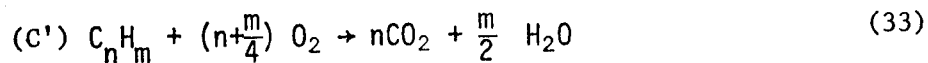
$$w_1 = B_1 \rho^{\alpha_1} T^{\alpha_2 + \alpha_3} \gamma_{HC}^{\alpha_2} \gamma_{O_2}^{\alpha_3} \exp(-E_1/T) \quad (30)$$

$$w_2 = B_2 \rho^{\beta_1} T^{\beta_2 + \beta_3 + \beta_5} \gamma_{CO}^{\beta_2} \gamma_{O_2}^{\beta_3} \gamma_{H_2O}^{\beta_5} \exp(-E_2/T) \quad (31)$$

and

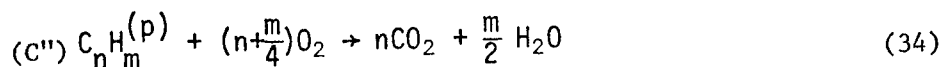
$$\gamma_{H_2O}(x) = \frac{m}{2} \frac{w_{H_2O}}{w_{HC}} \gamma_{HC}^{(o)} [\gamma_{THC}^{(o)} - \gamma_{THC}(x)] \quad (32)$$

Three global catalytic surface reactions are assumed to occur on the surface. They are:



with the corresponding surface rate J_3^* given by

$$J_3^* = C_3^* [C_n H_m]_s \exp(-E_3^*/RT_s^*)$$



$$\text{with } J_4^* = C_3^* [C_n H_m^{(p)}]_s \exp(-E_3^*/RT_s^*)$$



$$\text{with } J_5^* = C_4^* [CO]_s \exp(-E_4^*/RT_s^*)$$

Other equations are similar to those in Chapter I. The steady solution is obtained from the transient combustion code as discussed in Chapter I.

II.2 Computed Results

The design parameters of a catalytic combustor include the catalytic bed length, the after-bed reaction distance, the channel hydraulic diameter, the open area percentage, the catalyst variables (catalyst type, loading density, washcoat type) and staging arrangements (graded cell, for example). The operating parameters include inlet temperature and pressure, the approaching (reference) mixture velocity, the fuel/air equivalence ratio or the adiabatic flame temperature and fuel types. An exhaustive parametric study will not be practical for this report. Instead, selected computations are presented. Since emphasis is placed on automotive gas turbine application, we are most interested in higher inlet temperature, above atmospheric pressure and high reference velocity operations with thin substrate and large open area percentage design. The total combustor length (bed plus after-bed) required to meet the emission goal (13.6 g CO/kg fuel, 1.64 g THC/kg fuel) as a function of these parameters is the main output of the model calculation.

The chosen fuel is No. 2 Diesel which was used by Anderson (1977a, 1978, 1980a). Its hydrogen-carbon atom ratio is 1.8 with 27.55% aromatics. The molecular weight is taken to be 138 for the purpose of estimating the diffusion coefficient which is assumed to vary as one over the square root of molecular weight. Other properties can be found in Anderson (1977a). The catalytic combustor used for reference calculation is the one by Matthey Bishop which was also described by Anderson (1980a) (MBI-2.5 and MBI-5.4). The values of kinetic parameters are listed in Table II.1. Expressions in Reactions A" to D are taken from Edelman and Fortune (1969), Dryer and Glassman (1973), Marteney (1979) and Kuo and Morgan (1971) respectively, all with adjusted pre-exponential

Table II.1 Chemical Kinetic Constants
(for Chapter II)

Reaction (A')	Reaction (A'')	Reaction (B)	Reactions (C')(C'')	Reaction (D)
$C_0^* = 1.6 \times 10^6$	$C_1^* = 1.8 \times 10^5$	$C_2^* p_1^{\beta_1} = .54 \times 10^{14}$ (at 3 atm)	$C_3^* = 1.5 \times 10^4$	$C_4^* = 10^5$
$\gamma_1 = 0$	$\alpha_1 = 0.3$		$E_3^* = 10$ (kcal/mole)	$E_4^* = 17.8$ (kcal/mole)
$\gamma_2 = 0.5$	$\alpha_2 = 0.5$	$\beta_2 = 1$		
$\gamma_3 = 0$	$\alpha_3 = 1$	$\beta_3 = 0.25$		
	$\alpha_4 = 1$	$\beta_4 = 0$		
$E_0^* = 34$ (kcal/mole)	$E_1^* = 24$ (kcal/mole)	$\beta_5 = 0.5$		
		$E_2^* = 40$ (kcal/mole)		

factors. The calculated results are not very sensitive to catalytic kinetic parameters indicating mass transfer dominates the surface reactions. The choice of gas-phase hydrocarbon oxidation kinetic constants deserves some explanation, since kinetic rates for No. 2 Diesel fuel are hard to find. Ignition delay times as a function of initial temperature, however, do exist for long chain and cyclic hydrocarbons (Dryer and Glassman, 1978, Edelman, 1978), which are the ingredients of the Diesel fuel. The ignition delay time of No. 2 Diesel is assumed to be the arithmetic mean of its ingredients. Model calculations are then performed for pure gas phase reactions and the ratio of calculated hydrocarbons disappearance times as a function of initial temperature is taken to be proportional to the ratio of ignition delay times as indicated in Fig. II.1. This provides some measure for the correct temperature dependence in the gas kinetic parameters for the diesel fuel. The use of "hydrocarbon disappearance time" in this comparison reflects the difficulty of identifying ignition time in the theoretical study. The pre-exponential factor in reaction (B) is adjusted to fit the CO decay data of Anderson (1980a).

The model calculations for the catalytic combustors will be presented next.

Effects of Catalytic Bed Length, Downstream Reaction Distance,

Reference Velocity and Adiabatic Flame Temperature

Figure II.2 shows the detailed profiles of two cases; one with a 5-cm bed and the other with a 2.5-cm bed. If we look at the 5-cm case first, we see when mixture enters into the reactor channel, the fuel is quickly consumed on the surface by catalytic reaction, the surface temperature starts from a low value ($T_s = 1.106$), due to the fast heat and mass transfer rates at the entrance region, and rises sharply away from the channel entrance. The gas

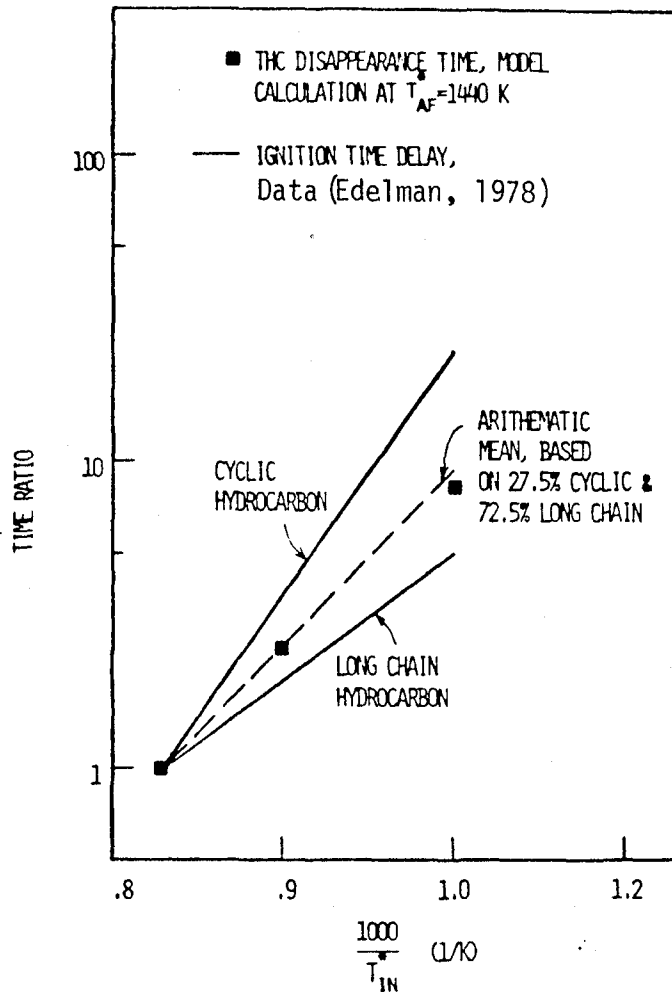


Fig. II.1 Comparison of temperature dependence for the computed disappearance time (nondimensional) of Diesel No. 2 fuel with Ignition Delay Data (Edelman, 1978). Reference time is taken at 1200 K.

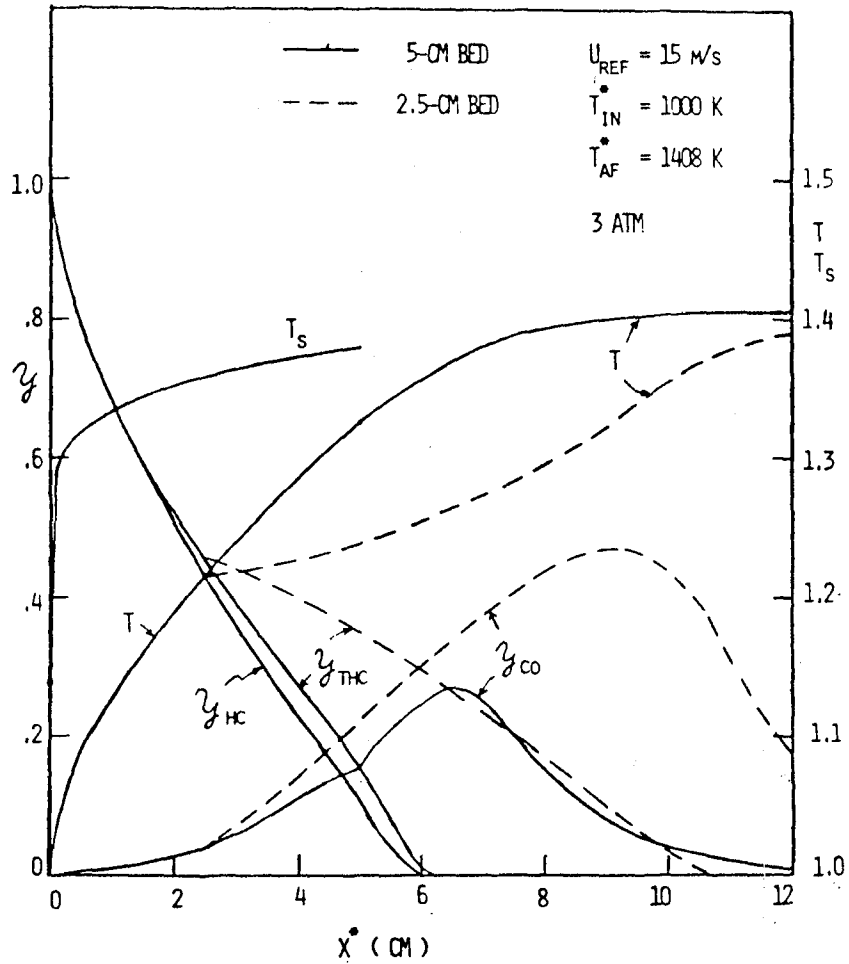


Fig. II.2 Computed temperature and species profiles for two similar catalytic combustors with different bed lengths, $A^*/A_T^* = 0.93$ and $d^* = 1.382 \text{ mm}$.

temperature begins to rise due to the heat transfer from the substrate and when T reaches 1.15, gas-phase reaction is initiated and the hydrocarbon fuel is converted to the "pyrolyzed hydrocarbon," which is equal to the difference between y_{THC} (total hydrocarbon) and y_{HC} (original hydrocarbon). At the same time, CO, which is produced only in the gas-phase, begins to rise. The carbon monoxide in turn is consumed by both gas-phase and surface reactions to form CO_2 until the bed exit is reached. After the exit, CO is consumed by gas-phase reaction only so a slope discontinuity of the CO curve occurs at $x^* = 5$ cm. Similar discontinuity can be found in temperature and hydrocarbons, although in the latter case, it is not very apparent. If at the bed exit the gas temperature is high enough, the gas-phase reaction will continue at a high rate and adiabatic flame temperature is reached at $x^* = 12$ cm. As shown in Fig. II.2, a CO peak occurs when its production and oxidation rates become equal.

If the catalytic bed is cut short at 2.5 cm. as shown in Fig. II.2, the total hydrocarbon (y_{THC}) oxidation rate decreases suddenly at the bed exit (2.5 cm) due to the absence of surface reaction. Since the gas temperature is not yet high enough, the gas-phase reaction downstream proceeds slowly as shown by the slower increase of gas temperature. Because a larger fraction of the hydrocarbon fuel has to be consumed in the gas-phase reaction, higher CO peak occurs and the total combustor length required to reach the emission goal is accordingly longer than the case with longer catalytic bed.

It was shown in Chapter I that the effects of catalytic bed length, after-bed distance, gas velocity and open area percentage could be correlated using reference gas residence times in the reactor bed and in the after-

bed space. For a fixed open area fraction, this correlation is simplified and can be expressed by the ratios of lengths over the reference velocity as given in Fig. II.3. For a fixed "gas residence time" in the bed (L^*/U_{ref}^*), there is a corresponding minimum combustor residence time (L_{EG}^*/U_{ref}^*) for emissions goals to be satisfied. Although the residence time correlation is natural for gas-phase reactions, it is less obvious for surface reactions. The validity of this type of correlation is independent of the gas kinetic schemes used as illustrated here and in Chapter I where two-step kinetics and different sets of catalytic parameters were employed.

Fig. II.3 shows that as the catalytic bed length increases, the required combustor length decreases. This may lead one to choose a design which is all reactor bed without the downstream gas reaction space. However, as discussed in Chapter I, in many catalytic combustor applications (e.g., transportation engines), a fast combustor response is required. Longer reactor bed results in a longer response time due to the larger substrate thermal inertia. Therefore, certain compromises may have to be made between steady and nonsteady considerations. Take Fig. II.3, for example, one may want to choose a bed residence time of 4 milliseconds instead of 6 milliseconds. This increases the total combustor length by 15% but reduces the response time by 30%. As the inlet temperature becomes higher, as preferred by the automotive gas turbine design, the required reactor bed will be drastically reduced, leaving most reactions to occur in the gas-phase. A shorter reactor bed also decreases the pressure loss.

The importance of downstream gas-phase reactions has been recognized by Anderson as demonstrated in much of his work (Anderson, 1977b, 1980a, T'ien and Anderson, 1979). Figure II.4 compares the model calculation with his recent data (Anderson, 1980a) on CO emission index as a function of downstream

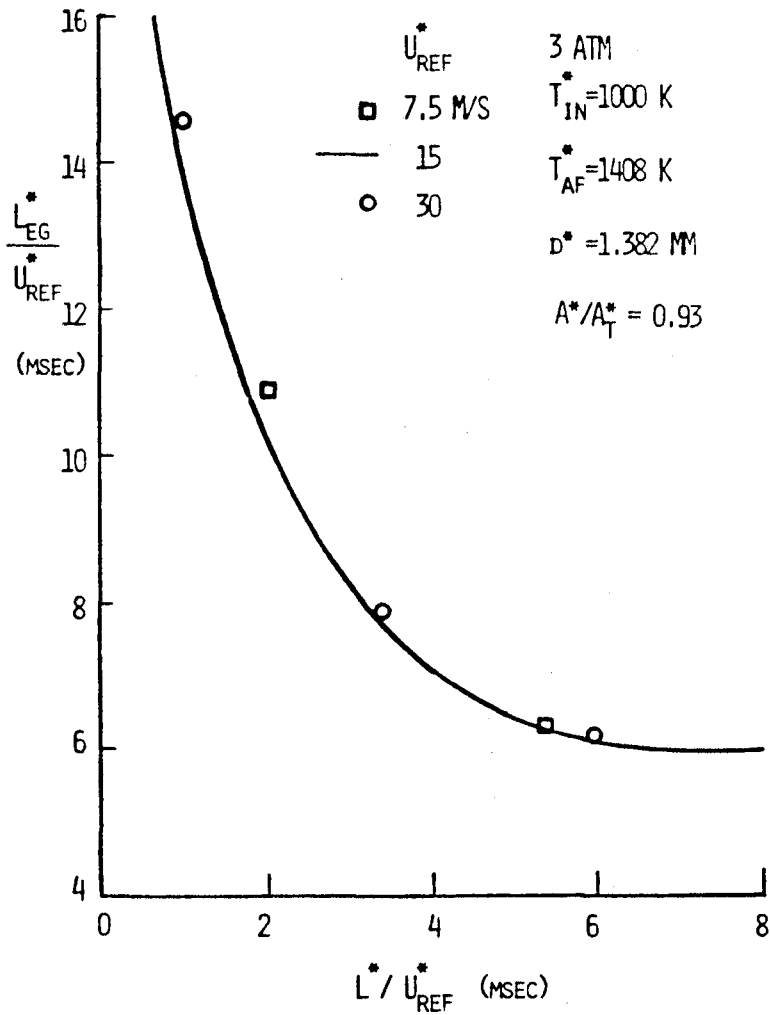


Fig. II.3 Computed "residence time" correlation: total residence time in combustor (bed plus after-bed) to reach emission goals vs. residence time in catalytic beds.

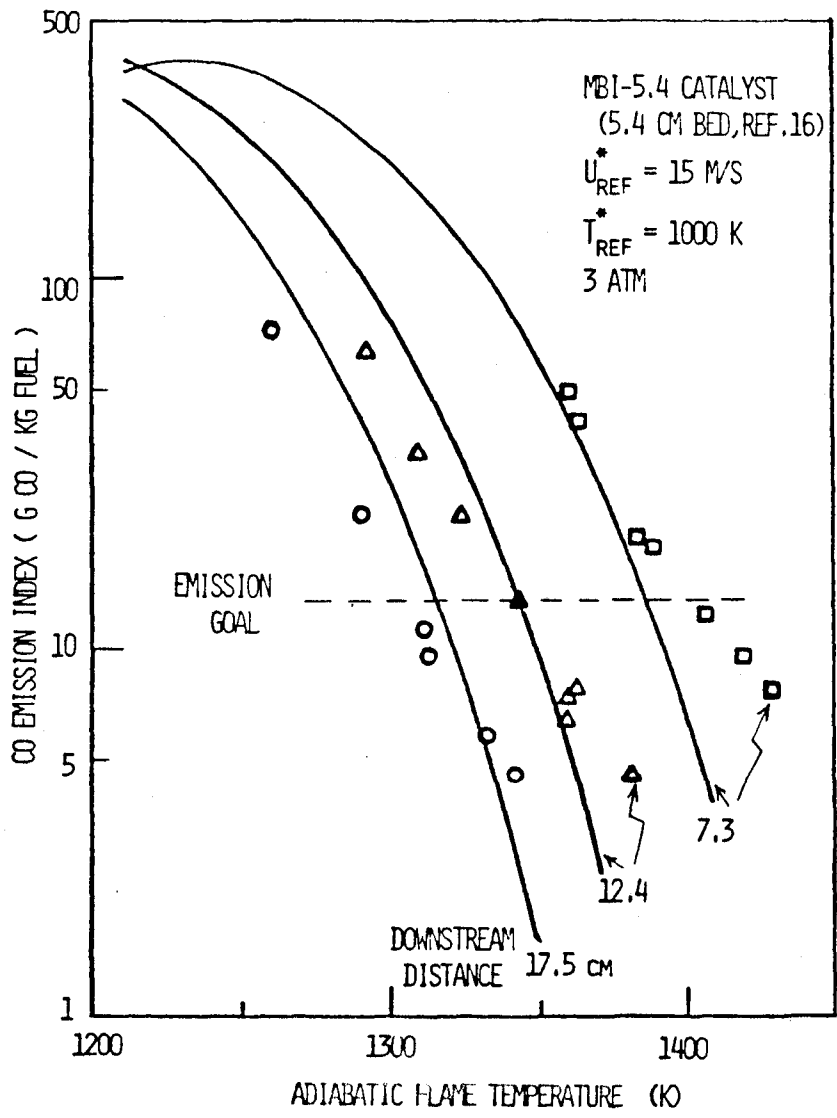


Fig. II.4 CO emission index vs. adiabatic flame temperature: comparison of model calculation with Anderson's data (1980a).

reaction distance and adiabatic flame temperature. Figure II.5 compares the minimum operating flame temperature vs. the downstream reaction distance for two bed lengths and two velocities. The comparison between the model and data is reasonably good within the range of parameters varied.

The appearance of CO peak as indicated in Fig. II.2 has been reported in previous experimental work (T'ien and Anderson, 1979, Bracco et al, 1980).

Effects of Inlet Temperature and Pressure

Figure II.6 shows the computed combustion efficiency as a function of adiabatic flame temperature for three inlet temperatures and two pressures at three different downstream locations. For a fixed pressure and adiabatic flame temperature, higher inlet temperature results in a higher efficiency at all three downstream positions. This is consistent with the experimental trend found by Anderson (1978). With higher inlet temperature, the gas-phase reaction is initiated earlier which results in a higher efficiency at a fixed location. However, as more residence time is given to the mixture, the difference in efficiency diminishes as can be seen from curves at different locations in Figure II.6.

From Fig II.6, for inlet temperature of 1000 K, the combustion efficiency at 3 atm is always higher than that at 6 atm. This is because of the faster mass diffusion rate at lower pressure. For 1100 K inlet temperature, however, a portion of the 6 atm efficiency curve is higher than that of the 3 atm case as can be seen in Fig. II.6(b) and (c). This reversal phenomenon was first reported by Anderson (1978) who suggested that this was due to the competition between gas-phase and surface reactions. This model calculation

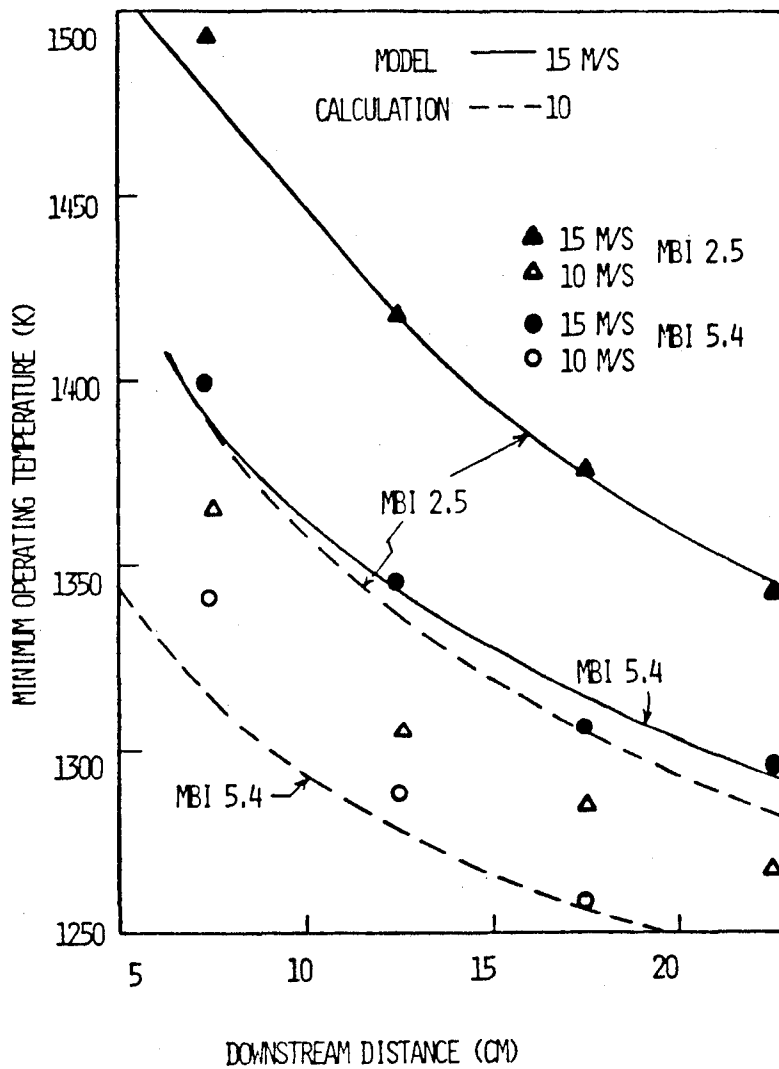


Fig. II.5 Minimum operating flame temperature (to reach emission goals) vs. downstream reaction distance: comparison of model calculation with Anderson's data (1980a).

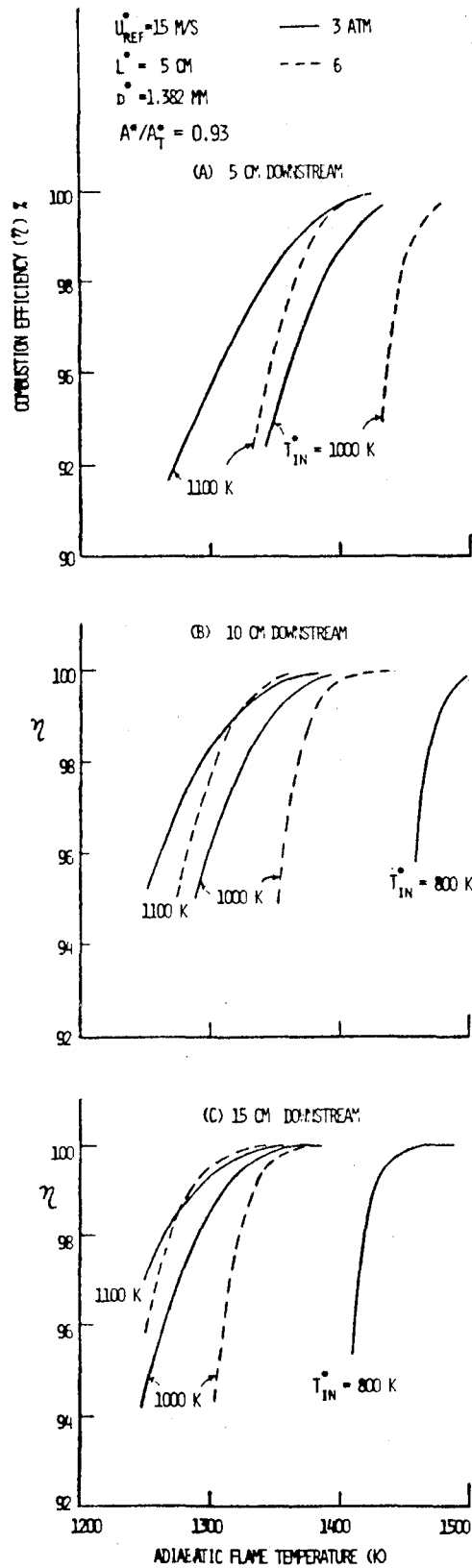


Fig. II.6 Combustion efficiency vs. adiabatic flame temperature for different inlet temperature and pressure at three downstream locations.

supports this interpretation. High temperature and pressure support fast gas-phase reactions, but high pressure also retards surface reaction through slower mass diffusion rate. Taking the case of 1100 K inlet temperature and 1320 K adiabatic flame temperature for example: at the bed exit, the 6 atm case has a lower efficiency than the 3 atm case because inside the reactor channel, surface reaction dominates. At downstream distance of 5 cm, the 6 atm case still has lower efficiency. But at 10 cm downstream, the two efficiencies become equal and at 15 cm downstream 6 atm has a higher efficiency. Since only gas-phase reaction exists in the after-bed space, the efficiency reversal occurs when the gas-phase reactions overpower the upstream influence of surface reactions.

SUMMARY

A transient model of monolith catalytic combustor is presented in this work. The model assumes a quasisteady gas phase and a thermally-thin solid with the substrate thermal inertia responsible for the combustor response time delay. In the gas-phase treatment, several quasi-global chemical reactions are assumed which are capable of describing CO and unburnt hydrocarbon emissions in fuel-lean operations. By neglecting heat conduction along the flow direction in the gas and the solid in high speed approaching flows, the system of differential equations describing the combustor transient is simplified and Runge-Kutta integration scheme is applicable. The resulting computation scheme is highly efficient in computational time and is suitable for parametric calculation for both steady states and transients.

In the steady-state computation presented, the influence of selected operating and design parameters on the minimum combustor length is studied. Special attention is given to the effect of after-bed gas phase reaction space. Comparison with the data by Anderson indicates that the model is able to describe all the salient features found in the experiments including the appearance of CO peak and the efficiency reversal phenomena at high inlet temperature and pressure. Quantitative agreement with CO emission data is possible if a certain degree of rate constants adjustment is made.

The model computation also suggests that for determining the condition of achieving the steady-state emission goals, the gas residence times in the catalytic bed and in the after-bed space are the similarity parameters absorbing the influence of catalytic bed and after-bed lengths, the gas velocity and the open area fraction of the catalytic element. Likewise, the nondimensional

response time and the gas residence times are the proper similarity parameters in transient operations. A consequence of this is that the dimensional response time is proportional to the substrate cross-sectional area A_s^* (all other parameters fixed) and so a thin substrate is necessary for fast response.

The computed time history provides an understanding of how a catalytic combustor responds to an upstream condition change. The leading edge of the substrate is the first to respond to an upstream variation, say, a change of fuel flow rate. The leading edge is closer to the source of variation and the mass transfer rate is higher in the flow entrance region of the gas channel. As a result, the surface fuel concentration is perturbed first which, through the surface reaction, produces a surface temperature change. Heat transfer across the flow channel then causes the gas temperature to vary and this disturbance propagates downstream by convection. Since, the downstream part of the substrate always responds to the upstream substrate temperature variation, it is not difficult to see from the above description that a combustor with a longer catalytic bed residence time will take a longer time to reach a new equilibrium state.

The model calculation also shows that higher combustor inlet temperature and adiabatic flame temperature shorten the response time. Smaller channel hydraulic diameter usually results in a faster response but there are exceptions. Since the requirements for faster transient response do not always coincide with the optimal steady-state design conditions, for applications where transient characteristics are important, both steady and transient studies have to be made simultaneously so that a good compromising design can be found.

References:

- Ablow, C.M. and Wise, H., (1979) "Theoretical Analysis of Catalytic Combustion in a Monolith Reactor," *Combustion Science and Technology*, 21, 35 (1979).
- Anderson, D.N., Tacina, R.R., and Mroz, T.S., (1975) "Performance of a Catalytic Reactor at Simulated Gas Turbine Combustor Operating Conditions," NASA TM X-71747.
- Anderson, D.N. (1976) "Preliminary Results from Screening Tests of Commercial Catalysts with Potential Use in Gas Turbine Combustors. Part I. Furnace Studies of Catalyst Activity," NASA TM-X 73410.
- Anderson, D.N., (1977a) "Performance and Emissions of a Catalytic Reactor with Propane, Diesel, and Jet A Fuels," NASA TM-73786.
- Anderson, D.N., (1977b) "Effect of Catalytic Reactor Length and Cell Density on Performance," presented at the 2nd EPA Workshop on Catalytic Combustion, Raleigh, N.C., June 21-22.
- Anderson, D.N., (1978) "Effect of Inlet Temperature on the Performance of a Catalytic Reactor," NASA TM-78977.
- Anderson, D.N., (1980a) "The Effect of Catalyst Length and Downstream Reaction Distance on Catalytic Combustor Performance," NASA TM-81475.
- Anderson, D.N., (1980b) "Ultra-lean Gas-phase Combustion," presented at the Automotive Technology Development Contractor Coordination Meeting, Dearborn, Michigan, November 11 - 13.
- Bracco, F.V., Bruno, C., Yaw, Y. and Walsh, P.M., (1980) "Computed and Measured Emissions from the Catalytic Combustion on Propane/Air Mixtures," Fourth Workshop on Catalytic Combustion, EPA-600/0-90-035.
- Cerkanowicz, A.E., Cole, R.B. and Stevens, J.G., (1977) "Catalytic Combustion Modeling: Comparison with Experimental Data," ASME paper, 77-GT-85.
- DeCorso, S.M. and Carl, D.E., (1979) "Structural Analysis of a Preliminary Catalytic Combustion Ceramic Design," Proceedings: Third Workshop on Catalytic Combustion, EPA-600/7-79-038.
- Dryer, F.L. and Glassman, I., (1973) "High Temperature Oxidation of CO and CH₄," 14th Inter. Symp. on Combustion, the Combustion Institute, Pgh., Pa.
- Dryer, F.L. and Glassman, I., (1978) "Combustion Chemistry of Chain Hydrocarbons," in Alternative Hydrocarbon Fuels: Combustion and Chemical Kinetics, Vol. 62, Progress in Astron. and Aeronautics. Also discussion section, p. 295.
- Edelman, R.J., (1978) Comments Section in the previous reference, p. 295.

- Edelman, R.B. and Fortune, O.F., (1969) "A Quasi-global Chemical Kinetic Model for Finite Rate Combustion of Hydrocarbon Fuels with Application to Turbulent Burning and Mixing in Hypersonic Engines and Nozzles," AIAA paper 69-86.
- Kays, W.M., (1966) Convective Heat and Mass Transfer, McGraw-Hill, New York.
- Kelley, J.T., Kendall, R.M., Chu, E. and Kesselring, J.P., (1977) "Development and Application of the PROF-HET Catalytic Combustor Code," paper presented at the 1977 Fall Meeting Western States Section, The Combustion Institute.
- Kendall, R.M. Kelley, J.T., Chu, E.K. and Kesselring, J.P., (1979) "An Analysis of Catalytic Combustion in Monolithic Honeycomb Beds," Proceedings: Third Workshop on Catalytic Combustion, EPA-600/7-79-038.
- Kuo, J.C.W. and Morgan, C.R., (1971) "Mathematical Models of the Monolith Catalytic Converter," SAE Transaction, V. 80, 1971, #710289.
- Martenev, P.J., (1979) "Determination of the Rate of Heterogeneous Reaction on Catalytic Surfaces," Proceedings: Third Workshop on Catalytic Combustion, EPA-600/7-79-038.
- Schwartz, A., Holbrook, L.L. and Wise, H., (1971) "Catalytic Oxidation Studies with Platinum and Palladium," Journal of Catalysts, 21, 199-207.
- T'ien, J.S., (1980) "Modeling of Transient Operation of Catalytic Combustor," Proceedings: Fourth Workshop on Catalytic Combustion, EPA-600/9-80-035.
- T'ien, J.S. and Anderson, D.N., (1979) "Gas Phase Oxidation Downstream of a Catalytic Combustor," NASA TM-81551.

Nomenclature

A^* cross-sectional area of one gas channel

A_s^* substrate cross-sectional area associated with one gas channel, see Fig. 1

$A_T^* = A^* + A_s^*$, total cross-sectional area of one cell unit

$$B_0 = \frac{L^*}{U^*(0)} \frac{1}{\rho^*(0)} \frac{1}{Y_{HC}(0)} C_0^* p^*(0)^{\gamma_1} \rho^*(0)^{\gamma_2} T^*(0)^{\gamma_3} Y_{HC}(0)^{\gamma_2} W_{HC}^{(1-\gamma_2)}$$

$$B_1 = \frac{L^*}{U^*(0,0)} \frac{1}{\rho^*(0,0)} \frac{1}{Y_{HC}(0,0)} C_1^* p^*(0,0)^{\alpha_1} \rho^*(0,0)^{(\alpha_2+\alpha_3)} T^*(0,0)^{\alpha_4} Y_{HC}(0,0)^{\alpha_2} Y_{O_2}(0,0)^{\alpha_3} \\ \times W_{HC}^{(1-\alpha_2)} W_{O_2}^{-\alpha_3}$$

$$B_2 = \frac{L^*}{U^*(0,0)} \frac{1}{\rho^*(0,0)} \frac{1}{Y_{HC}(0,0)} C_2^* p^*(0,0)^{\beta_1} \rho^*(0,0)^{(\beta_2+\beta_3+\beta_5)} T^*(0,0)^{\beta_4} Y_{HC}^{\beta_2}(0,0) \\ \times Y_{O_2}^{\beta_3}(0,0) W_{CO}^{(1-\beta_2)} W_{O_2}^{-\beta_3} W_{H_2O}^{-\beta_5}$$

$$B_3 = C_3^* d^* / \alpha^* W_{HC} Nu_{\infty}$$

$$B_4 = C_4^* d^* / \alpha^* W_{CO} Nu_{\infty}$$

$$C_n = n W_{CO} / W_{HC}$$

C_s^* specific heat of substrate

C_p^* gas specific heat

d^* catalytic monolith combustor channel equivalent diameter

d_s^* half thickness of the substrate

E^* activation energy

J_3^* mass consumption rate of hydrocarbons per unit surface area through reaction (C)

J_4^* mass consumption rate of CO per unit surface area through reaction (D)

$$J_{Di} = J_H (Le_i)^{2/3}$$

$$J_H = 4 Nu_x (\alpha^*(0,0)/d^{*2}) (L^*/u^*(0,0)) (k^*/k^*(0,0))$$

k^* heat conductivity of the gas
 L^* catalytic bed length
 L_{as}^* length of after-bed downstream gas phase reaction space
 L_c^* total combustor length (catalytic reactor length plus after-bed downstream gas reaction distance)
 L_{EG}^* total combustor length (catalytic bed plus after-bed space) required to meet emission goals
 Le_1 Lewis number for hydrocarbon gas in air
 Le_2 Lewis number for CO in air
 m number of hydrogen atom in $C_n H_m$
 n number of carbon atom in $C_n H_m$
 Nu_x Nusselt number at x
 Nu_∞ Nusselt number for fully developed flow
 $p = p^*/p^*(0,0)$, nondimensional pressure
 $q_1 = q_1^*/C_p^*T^*(0,0)$, nondimensional heat of combustion per unit mass of $C_n H_m$ in reaction A
 $q_2 = q_2^*/C_p^*T^*(0,0)$, nondimensional heat of combustion per unit mass of CO in reaction B
 $q_3 = q_3^*/C_p^*T^*(0,0)$, nondimensional heat of combustion per unit mass of $C_n H_m$ in reaction C
 $q_4 = q_4^*/C_p^*T^*(0,0)$, nondimensional heat of combustion per unit mass of CO in reaction D, same as q_2
 r_{nk} see Eq. (17)
 S^* circumferential length of one channel crosssection ($= \pi d^*$)
 $T = T^*/T^*(0,0)$, nondimensional gas temperature
 $T_s = T_s^*/T^*(0,0)$, nondimensional substrate temperature

T_{af}^* adiabatic flame temperature
 T_{in}^* combustor inlet temperature
 t = t^*/τ^* , nondimensional time
 t_b^* = $(L^*/U_{ref}^*) (A^*/A_T^*)$, reference gas residence time in the catalytic combustor bed
 t_{as}^* = L_{as}^*/U_{ref}^* , reference gas residence time in the after-bed space
 t_{ch}^* characteristic transient response time ($\eta_T \rightarrow 80\%$)
 t_{EG}^* Minimum total combustor gas residence time ($t_b^* + t_{as}^*$) needed to reach emission goals
 u = $u^*/u^*(0,0)$, nondimensional flow velocity
 u_{ref}^* reference gas velocity, measured at upstream of catalytic bed
 W_i molecular weight of species i
 w_i chemical reaction rate
 x = x^*/L^* , nondimensional axial distance measured from catalytic bed entrance to downstream
 Y_i mass fraction of species i
 γ_{CO} = $Y_{CO}/Y_{HC}^{(0,0)}$
 γ_{O_2} = $Y_{O_2}/Y_{O_2}^{(0,0)}$
 γ_{HC} = $Y_{HC}/Y_{HC}^{(0,0)}$
 $\gamma_{HC}^{(p)}$ = $Y_{HC}^{(p)}/Y_{HC}^{(0)}$
 γ_{THC} = $\gamma_{HC} + \gamma_{HC}^{(p)}$

α^*	thermal diffusivity of gas
α_i	rate exponent, see Eqs (1) and (23)
β	rate constant, see Eq. (22)
β_i	rate exponent, see Eqs (2) and (24)
γ_i	rate exponent, see Eq (22)
ρ^*	gas density
ρ_s^*	substrate density
τ^*	characteristic substrate heat-up time, see Eq. (16)
η_{CB}	carbon-balanced efficiency
η_T	combustion efficiency based on temperature difference
[]	concentration, g-mole/c.c.

Subscript

s surface

Superscript

* dimensional quantity

APPENDIX I

LISTING OF COMPUTER PROGRAMS FOR CHAPTER I

The numerical computations were performed using an interactive VAX - 11/780 computer. FORTRAN language was used in writing the main program (e.g. IGNITION. FOR; 17) and the data program (e.g. BLOCK. FOR; 31). They were then compiled to form the objective programmes (e.g. IGNITION. OBJ; ** and BLOCK. OBJ; **). The two objective programmes were then linked together to form an executable program (e.g. IGNITION. EXE; 10). In performing a calculation, only the executable is needed.

The BLOCK program stores most of the data which are not likely to be changed from one calculation to the other, while the most frequently varied input data will be read in in each computer run. If the data stored in the BLOCK program are to be changed, the FORTRAN BLOCK program has to be modified (edited), re-compiled and linked with the main program to form a new executable program.

In the following, the FORTRAN programmes (IGNITION. FOR; 17 and BLOCK. FOR; 31) are listed together with a sample calculation showing input and output data.

The IGNITION program is presently set up to perform the start-up transient. With minor modification, it can read in any prescribed initial condition and to calculate the corresponding unsteady response. Given enough computational time, the IGNITION program will also result in the steady-state profiles.

More detailed instructions (for IGNITION. FOR; 17):

1. The number of grid points used should be less than 300. If more than 300 points are needed, line 600 has to be changed.
2. Read-in data (lines 10900 - 12300):
XPHI = ϕ = fuel-air equivalence ratio

TI = T (0,0) = upstream, initial temperature (K)

XPI = P(0,0) = upstream, initial pressure (Atm.)

UIUS = U_{ref} = upstream (outside of the bed) initial gas velocity (m/s)

XLS = reference length (m), suggested to use 0.1 m (10 cm)

DS = d^* = channel hydraulic diameter (m)

AOAS = A^*/A_s^* = open-to-close area ratio

D_X = nondimensional step size in X (space). It is nondimensionalized by XLS. So if XLS = 0.1 m and $DX = 0.01$, dimensional step size is 0.001 m or 1 mm.

DT = nondimensional time step size

TMAX = maximum nondimensional time allowed for computation

IPRINT = time interval for printing out transient profiles.

For example, if $DT = .01$ and $IPRINT = 25$,

Output will be printed out every $t = 0.25$.

N = number of grid points (in X direction) in the catalytic bed. The nondimensional catalytic bed length is given by $(N-1) \times (DX)$. For example, if $N = 51$, $DX = .01$, then the nondimensional bed length is equal to 0.5. If XLS = .1 m, then the dimensional bed length is .05 m (5 cm).

NAS = number of grid points (in X-direction) in the downstream after-bed space. The length of the downstream distance can be calculated in a similar manner as in the above.

$C_1, C_2, C_3, C_4 = C_1, C_2, C_3, C_4$ (See Table I.2)

IT = interval in X for printout. For example, if $DX = 0.01$

IT = 5, the printout will be at $X = 0, 0.05, 0.1, 0.15, \dots$
etc.

3. Those data which are not read in will be defined by the BLOCK program.

4. Some Symbol Definitions:

PR = Prandtl number of air

REY = Reynolds number based on channel diameter and
upstream velocity

ES,S = E_1^* , E_2^* , E_3^* , E_4^* (See Table I.2)

E,S = E_1 , E_2 , E_3 , E_4

C,S = C_1^* , C_2^* , C_3^* , C_4^* (See Table I.2)

GC = gas constant (joule/kg K)

XLEW1 = Lewis number for $C_n H_m$ in mixture

XLEW2 = Lewis number for CO in mixture

ROI = initial, upstream (I.U.) gas density (kg/m^3)

XKI = I.U. gas heat conductivity (cal/m sec K)

CP = specific heat of gas at constant pressure (cal/kg K)

ALPHA = I.U. gas diffusivity (m^2/sec)

TS = T_s

YFS = $y_{HC,s}$

YCS = $y_{CO,s}$

YO = y_{O_2}

YF = y_{HC}

TMAX = Maximum time for computation

YC = y_{CO}

5. Output data (lines 40300 to 42200)

The following quantities are printed out as a function
of axial distance and time:

Nondimensional gas and surface temperatures, Emission
indices ($\times 1000$) of hydrocarbon fuel and CO (both in the gas
phase and on the surface) and carbon-balanced and thermal
efficiencies.

```

100 C *****
200 C *****CATALYTIC COMBUSTOR START-UP TRANSIENT*****
300 C *****
400 C *****
500 C
600 C PARAMETER NX=300
700 COMMON /ACTI/ES1,ES2,ES3,ES4
800 COMMON /MOLEQ/ WHC, WCO, WO2, WH2O
900 COMMON /TH1/XM, XM, G1S, Q2S
1000 COMMON /TH2/ CP, GC, XPR
1100 COMMON /UPS1/ YCI, YCI
1200 COMMON /IN1/TS, YFS, YCS
1300 C
1400 C DIMENSION YF(NX), T(NX), TS(NX), YO(NX), YFS(NX), RC(NX), U(NX)
1500 C DIMENSION XKY(4), XK1(4), XKTS(4), XKC(4), YC(NX), YCS(NX)
1600 C DIMENSION XJH(NX), XJD1(NX), XJD2(NX), YH2C(NX), XP(NX)
1700 C DIMENSION EFF(NX), RNK(NX), EFFT(NX)
1800 C
1900 C 7 FORMAT (4E20.10)
2000 C 8 FORMAT (I4)
2100 C 9 FORMAT (1H0,'SLID TEMPERATURE (TS)')
2200 C 10 FORMAT (6F12.6)
2300 C 11 FORMAT (1H0,'SURFACE HC MASS FRACTION (YFS)')
2400 C 12 FORMAT (//)
2500 C 13 FORMAT (1H0,'GAS TEMPERATURE (T)')
2600 C 14 FORMAT (1H0,'CNHM MASS FRACTION (YF)')
2700 C 15 FORMAT (1H0,'YCO(UPST,INI) =',F10.6,5X,'YF(UPST,INI) =',F10.7
2750 C 1,5X,'EQUIL RATIO =',F15.9//)
2800 C 17 FORMAT (1H0,'G1 =',F15.7,5X,'G2 =', F15.7,5X,'DX =',F15.7,5X,'DT =',
2900 C 1F15.7//)
3000 C 18 FORMAT (1H0,'N =',I10//)
3100 C 19 FORMAT (1H0,'INITIAL CONDITIONS (TS)')
3200 C 20 FORMAT (1H0,'TMAX =',F15.8)
3300 C 21 FORMAT (1H0,'NC, OF GRID POINT =',I21//)
3400 C 22 FORMAT (1H0,'TIME =',F15.8,5X,'KOUNT =',I10//)
3500 C 23 FORMAT (//)
3600 C 24 FORMAT (10E12.5)
3700 C 25 FORMAT (1H0,'INITIAL CONDITIONS (YFS)')
3800 C 26 FORMAT (1H0,'XJH')
3900 C 31 FORMAT (1H0,'CO MASS FRACTION (YC)')
4000 C 32 FORMAT (1H0,'SURFACE CO MASS FRACTION (YCS)')
4100 C 33 FORMAT (1H0,'INITIAL CONDITIONS (YCS)')
4200 C 34 FORMAT (1H0,' ES, S =',6F12.6//)
4300 C 35 FORMAT (1H0,' C, S =',4E20.10//)
4400 C 36 FORMAT (1H0,' A, S =',6F12.6//)
4500 C 37 FORMAT (1H0,' PE, S =',6F12.6//)
4600 C 41 FORMAT (1H0,' YCO =',//)
4700 C 42 FORMAT (1H0,' YCO(SURFACE) =',//)
4800 C 43 FORMAT (1H0,' L/U =',F15.7//)
4900 C 44 FORMAT (1H0,' B1S, B2S, =',4E15.8//)
5000 C 45 FORMAT (1H0,' B1, B2, B3, B4 =',4E15.8//)
5100 C 46 FORMAT (4E20.8)
5200 C 47 FORMAT (1H0,' E, S =',6F12.6//)
5300 C 48 FORMAT (1H0,' GC, XLEW1, XLEW2, XLS, DS =',6F12.6//)
5400 C 49 FORMAT (1H0,' RCI, XK1, CP, ALPHA =',3F12.6,E12.5//)
5500 C
5600 C
5650 C
5700 C 71 FORMAT (1H0,'APPROACH VEL =',F10.4//)
5800 C 72 FORMAT (1H0,'CHANNEL VEL (I.U.) =',F10.5//)
5900 C 73 FORMAT (1H0,'EFFICIENCY(CARBON-BALANCE)')
6000 C 74 FORMAT (1H0,'EFFICIENCY(TEMPERATURE)')
6100 C 401 FORMAT (1H0,' XFI =',F20.5//)
6200 C 402 FORMAT (1H0,' TI, PR, REY, AD2UL, ADAS =',5F12.5//)
6300 C 403 FORMAT (1H0,' ES, S =',4E20.8//)
6400 C 404 FORMAT (1H0,'*****',//)
6500 C 405 FORMAT (1H0,'GAS TEMPERATURE IS NEGATIVE')
6600 C 406 FORMAT (1H0,'CNHM CONCENTRATION IS NEGATIVE')
6700 C 407 FORMAT (1H0,'CO CONCENTRATION IS NEGATIVE')
6800 C 408 FORMAT (1H0,'YFF IS NEGATIVE')
6900 C 409 FORMAT (1H0,'ADIABATIC FLAME TEMP =',F10.6//)
7000 C 410 FORMAT (1H0,'ADIAB FLAME TEMP(K) =',F15.5//)
7100 C
7200 C *****
7300 C *****
7400 C *****INPUT PARAMETERS*****
7500 C *****
7600 C *****CHEMICAL PARAMETERS*****
7700 C *****
7800 C *****
7900 C *****
8000 C *****
8100 C *****
CHEMICAL REACTION 1, CNHM + C2 = CO + H2C (GAS PHASE)
CHEMICAL REACTION 2, CO + O2 = CO2 (GAS PHASE)
CHEMICAL REACTION 3, CNHM + O2 = CO2 + H2C (SOLID SURFACE)

```

```

8200 C CHEMICAL REACTION 4, CO +O2 = CO2 (SOLID SURFACE)
8300 C
8400 C
8500 C ES1 = ACTIVATION ENERGY FOR REACTION 1 (CAL/MOLE),ETC.
8600 C C1 = PREEXPONENTIAL FACTOR (DIMENSIONAL) FOR REACTION 1, ETC.
8700 C WHC, WCU = MOLECULAR WEIGHTS FOR CNHM, CU
8800 C Q1S = HEAT OF COMBUSTION FOR REACTION 1 (CAL/G OF CNHM)
8900 C Q2S = HEAT OF COMBUSTION FOR REACTION 2 (CAL/G OF CU)
9000 C Q3S = HEAT OF COMBUSTION FOR REACTION 3 (CAL/G OF CNHM)
9100 C
9200 C XN = THE NUMBER OF CARBONS IN CNHM
9300 C XM = THE NUMBER OF HYDROGEN IN CNHM
9400 C
9500 C
9600 C
9700 C QS = Q1S + Q2S*XN*WCC/WHC
9800 C
9900 C ***** CATALYTIC BED PARAMETERS *****
10000 C
10100 C XLS = BED LENGTH (M)
10200 C DS = CHANNEL HYDRAULIC DIAMETER (M)
10300 C SOA = CIRCUMFERENTIAL LENGTH DIVIDED BY CHANNEL AREA,=4/DS(1/M)
10400 C AOAS = RATIO OF OPEN TO CLOSED AREAS
10500 C CSS = HEAT CAPACITY OF SUBSTRATE (CAL/KG/K)
10600 C ROS = DENSITY OF SUBSTRATE (KG/M3)
10700 C
10800 C
10900 C READ (5,10) XPH1
11000 C READ (5,10) TI
11100 C READ (5,10) XPI
11200 C READ (5,10) UIUS
11300 C READ (5,10) XLS
11400 C READ (5,10) DS
11500 C READ (5,10) ACAS
11600 C READ (5,10) DX
11700 C READ (5,10) CI
11800 C READ (5,10) TMAX
11900 C READ (5,8) IPRINT
12000 C READ (5,8) N
12100 C READ (5,8) NAS
12200 C READ (5,*) C1,C2,C3,C4
12300 C READ (5,8) IT
12400 C SGA = 4.0/DS
12500 C CN = XN*WCC/WHC
12600 C NPNAS = N + NAS
12700 C
12800 C ***** OPERATING PARAMETERS *****
12900 C TI = INITIAL, UPSTREAM (I.U.) TEMPERATURE (K)
13000 C UI = I.U. VELOCITY (M/S)
13100 C XPI = I.U. PRESSURE (ATM.)
13200 C RCI = I.U. GAS DENSITY (KG/M3)
13300 C YFI = I.U. MASS FRACTION OF HC
13400 C YCI = I.U. MASS FRACTION OF CC
13500 C YOI = I.U. MASS FRACTION OF C2
13600 C XPHI = UPSTREAM HC/O2 EQUIVALENCE RATIO
13700 C
13800 C
13900 C
14000 C UI = UIUS*(1.0+OAS)/AOAS
14100 C XMU = 0.000001458*SQRT(TI)/(1.0+110.4/TI)
14200 C YFI = WHC*XPHI/29./((XN+XM/4.)*4.76+XPHI)
14300 C XLEW1 = 1.5* SQRT (29./WHC)
14400 C XLEW2 = 1.5* SQRT (29./WCC)
14500 C XLE123=XLEW1**.667
14600 C XLE223=XLEW2**.667
14700 C
14800 C XLGU = XLS/UI
14900 C
15000 C ***** GAS PROPERTY *****
15100 C
15200 C CP = SPECIFIC HEAT OF GAS (CAL/KG/K)
15300 C XKI = HEAT CONDUCTIVITY OF GAS AT I.U. (CAL/M/SEC/K)
15400 C ALPHA = I.U. GAS THERMAL DIFFUSIVITY (M2/SEC)
15500 C GC=GAS CONSTANT FOR GAS MIXTURE (JOULE/KG/K)
15600 C XLEW1 = LEWIS NUMBER FOR CNHM IN MIXTURE
15700 C XLEW2 = LEWIS NUMBER FOR CO IN MIXTURE
15800 C
15900 C
16000 C XKI=.003+.000013*TI
16100 C ROI = XPI/GC/TI
16200 C ALPHA = XKI/RCI/CP

```

```

16300 REY = UIUS*DS*RCI/XMU
16400
16500
16600 TO DESCRIBE CHEMICAL REACTION RATE EXPRESSIONS
16700 REACTION 1 (GAS PHASE)
16800 D(CNHM)/DT $$$ XP**3*T*SQRT(YHC)*YO2/EXP(E1/RT)
16900
17000 REACTION 2 (GAS PHASE)
17100 D(CCC)/DT $$$ YCC*SQRT(YG2)*SQRT(YH2C)/EXP(E2/RT)
17200
17300 REACTION 3 (SOLID SURFACE)
17400 D(CNHM)/DT $$$ YHCS/EXP(E3/RT)
17500
17600 REACTION 4 (SOLID SURFACE)
17700 D(CCC)/DT $$$ YCCS/EXP(E4/RT)
17800
17900 TO EVALUATE KINETIC RATE CONSTANTS
18000
18100 B1SS = C1*SQRT(WHC)/WC2/SQRT(1000.)
18200 B1S = B1SS*XPI**3*RCI*SQRT(RCI)*TI*SQRT(YFI)*YO1
18300 B1 = XLOU*B1S/RCI/YFI
18400 SS*W2=SQRT(SQRT(WO2))
18500
18600 B2SS = C2/1000.**.75/SS*W2/SQRT(WH2C)
18700 SSRCI = SQRT(SQRT(ROI))
18800 SSYCI=SQRT(SQRT(YOI))
18900 B2S=B2SS*ROI*RCI/SSRCI*YFI*SSYOI
19000 R2 = B2S*XLOU/RCI/YFI
19100
19200 B3 = C3*DS/ALPHA/WHC/3.66
19300 B4 = C4*DS/ALPHA/WCO/3.66
19400 Q1 = Q1S/CP/TI
19500 Q2 = Q2S/CP/TI
19600 Q = QS/CP/TI
19700 TAB = YFI*Q+1.0
19800 TABDM = TAB*TI
19900 E1 = ES1/TI/1.987
20000 E2 = ES2/TI/1.987
20100 E3 = ES3/TI/1.987
20200 E4 = ES4/TI/1.987
20300 AD2UL = (ALPHA/DS/DS)/(UI/XLS)
20400 *****
20500
20600 WRITE (6,21) N,NAS
20700 WRITE (6,20) I*MAX
20800 WRITE (6,15) YCI, YFI, XPHI
20900 WRITE (6,71) UIUS
21000 WRITE (6,72) UI
21100 WRITE (6,17) Q1, Q2, DX, DT
21200 WRITE (6,402) TI, XPK, REY, AD2UL, AOAS
21300 WRITE (6,409) TAB
21400 WRITE (6,410) TABDM
21500 WRITE (6,403) ES1, ES2, ES3, ES4
21600 WRITE (6,47) E1, E2, E3, E4
21700 WRITE (6,35) C1, C2, C3, C4
21800 WRITE (6,48) GC, XLEW1, XLEW2, XLS, DS
21900 WRITE (6,49) RCI, XKI, CP, ALPHA
22000 WRITE (6,401) XPI
22100 WRITE (6,43) XLCU
22200 WRITE (6,44) B1S, B2S
22300 WRITE (6,45) B1, B2, B3, B4
22400 WRITE (6,19)
22500 WRITE (6,24) (TS (I), I=1,N,IT)
22600 WRITE (6,25)
22700 WRITE (6,24) (YFS(I), I=1,N,IT)
22800 WRITE (6,33)
22900 WRITE (6,24) (YCS(I), I=1,N,IT)
23000
23100 *****
23200
23300 ***** UPSTREAM CONDITICNS *****
23400 YF(1) = 1.
23500 YC(1) = 0.0
23600 YO(1) = 1.
23700 T(1) = 1.
23800 RO(1) = 1.
23900 XP(1) = 1.0
24000 U(1) = 1.
24100
24200 *****
24300

```

```

24400 C *****
24500 C START OF INTEGRATION LOOP
24600 KOUNT = 1
24700 XNUO = .885*SQRT(ADAS)*SQRT(XPR*RFY)
24800 ROCT1 = 0.0
24900 ROCT2 = 1.0
24950 555 CONTINUE
25000 ROOT = .5*(ROCT1 + ROCT2)
25100 IF(ROCT.LE.0.1)YNU=.0444/ROCT+3.46-1.34*ROCT
25200 IF(ROCT.GT.0.1)YNU=0.011/ROCT+3.66
25300 YROCT=YNU-XNUO
25400 IF (ABS(YROCT).LT.0.01) GO TO 200
25500 IF (YROCT.GT.0.0) ROCT1=ROOT
25600 IF (YROCT.LE.0.0) ROCT2=ROOT
25700 GO TO 555
25800 200 CONTINUE
25900 DMASS=RO(1)*U(1)
26000
26100 C
26200 C INTEGRATION OF QUASI-STEADY GAS PHASE EQUATIONS FOR
26300 C YF (FUEL MASS FRACTION) AND T (TEMPERATURE) IN DOWNSTREAM
26400 C DIRECTION USING FOURTH-ORDER RUNGE-KUTTA SCHEME
26500 C I IS THE INDEX FOR DOWNSTREAM DISTANCE X
26600 C
26700 DD 201 I=1, NPNAS
26800 C
26900 IF(I.GT.N)DMASS=RO(1)*U(1)*ACAS/(ACAS+1.)
27000 *****
27100 C
27200 C EVALUATE XJH AND XJD AS A FUNCTION OF X
27300 C
27400 C *****
27500 C NONDIMENSIONAL HEAT CONDUCTIVITY
27600 XK = (.003 + 0.000013* T1 *T(I))/X*I
27700 C *****
27800 C
27900 IF(I.GT.1) GO TO 180
28000 IF(I.EQ.1) X=0.0
28100 GO TO 181
28150 180 CONTINUE
28300 IX=I+1
28400 XI=IX-1
28500 X = XI*DX
28600 181 CONTINUE
28700 XST = X*2.0*AD2UL*XK+ROOT
28800 IF (XST.LE.0.1) XNU=0.0444/XST+3.46-1.34*XST
28900 IF (XST.GT.0.1) XNU=0.011/XST +3.66
29000 RNK(I)=XNU*XK/3.66
29100 XJH(I) = 4.0*XNU *AD2UL*XK
29200 IF (I.GT.N) XJH(I) = 0.0
29300 XJD1(I) = XJH(I) *XLE123
29400 XJD2(I) = XJH(I) *XLE223
29500 C *****
29600 C
29700 C 132 CONTINUE
29800 M=1
29900 DO 120 L=1,4
30000 IF (M.NE.1) GO TO 102
30100 YFF = YF(I)
30200 YCC = YC(I)
30300 TT = T(I)
30400 M = M+1
30500 GO TO 119
30600 102 CONTINUE
30700 IF (M.NE.2) GO TO 103
30800 YFF=YF(I)+DX*XKY(1)/2.
30900 YCC = YC(I) +DX*XKC(1)/2.
31000 TT=I(I)+XKI(1)*DX/2.
31100 M=M+1
31200 GO TO 119
31300 103 CONTINUE
31400 IF(M.NE.3) GO TO 104
31500 YFF = YF(I) + DX*XKY(2)/2.
31600 YCC = YC(I) + DX*XKC(2)/2.
31700 TT=I(I)+DX*XKI(2)/2.
31800 M=M+1
31900 GO TO 119
32000 104 CONTINUE
32100 YFF = YF(I) + DX*XKY(3)
32200 YCC = YC(I) + DX*XKC(3)
32300 TT=I(I) +DX*XKI(3)

```

```

32400 C 119 CONTINUE
32500 YH2C = MASS FRACTION OF H2O
32600 YH2C(I) = .5*XM*WH2C*YFI* (YF(1)-YF(1))/WHC
32650 IF(YFF.LT.0.0) YFF=0.0
32700 W1 = B1*XF(I)**.3*RC(I)*SQRT(RO(I))*T(I)*SQRT(YFF)*YC(I)
32800 1/EXP(E1/TT)
32900 SSYC=SQRT(SQRT(YU(I)))
33000 RO175=RO(I)*KG(I)/SQRT(SQRT(KC(I)))
33100 W2=B2*RG175*YCC*SSYC*SQRT(YH2C(I))/EXP(E2/TT)
33200 XKY(L) = -XJD1(I) *(YFF- YFS(1))/DMASS -W1/DMASS
33300 XKC(L) = -XJD2(I) *(YCC-YCS(1))/ DMASS +CN*W1/LMASS -W2/DMASS
33400 XKT(L) =-XJH(I)*(TT-TS(I))/DMASS+O1*YFI*W1/DMASS+O2*YFI*W2/DMASS
33500 120 CONTINUE
33600 YF(I+1) =YF(I) +DX*(XKY (1)/6. +XKY (2)/3. +XKY (3)/3.+XKY (4)/6.)
33700 IF (YF(I+1).LT.0.0) YF(I+1) =0.0
33800 YC(I+1)=YC(I)+DX*(XKC(1)/6.+XKC(2)/3.+XKC(3)/3.+XKC(4)/6.)
33900 IF (YC(I+1).LT.0.0) YC(I+1) =0.0
34000 T (I+1) =T (I) +DX*(XKT (1)/6. +XKT (2)/3. +XKT (3)/3.+XKT (4)/6.)
34100 IF (T(I+1).LT.0.0) GC TO 601
34200 ADD=YC(I+1)*YFI*W2/YCI/WCO/2.
34300 YO(I+1) =1.0-XFHI*(1.0-YF(I+1))+ADD
34400 XP(I+1)=XP(I)
34500 RO(I+1)=XP(I+1) /T(I+1)
34600 U(I+1) =DMASS/T(I+1)
34700 EFF(I)=1.-YF(I)-YC(I)*O2/O
34800 EFFI(I)=(T(I)-T(1))/(TAB-T(1))
34900 201 CONTINUE
35000 C
35100 C END OF ONE RUNGE-KUTIA INTEGRATION CYCLE FOR QUASI-STEADY
35200 C GAS PHASE EQUATIONS
35300 C *****
35400 C
35500 C *****
35600 C INTEGRATION OF UNSTEADY SOLID HEAT TRANSFER EQUATION
35700 C FOR TS (SOLID TEMPERATURE) IN TIME USING FOURTH-ORDER
35800 C RUNGE-KUTIA SCHEME
35900 C
36000 C
36100 C
36200 C
36300 DC 301 J =1,N
36400 MJ=1
36500 DC 320 LJ=1,4
36600 IF (MJ.NE.1) GC TO 302
36700 TSS =TS(J)
36800 MJ=MJ+1
36900 GO TO 319
37000 302 CONTINUE
37100 IF(MJ.NE.2) GO TO 303
37200 TSS = TS(J) + DT*XKTS(1)/2.
37300 MJ=MJ+1
37400 GO TO 319
37500 303 CONTINUE
37600 IF(MJ.NE.3) GO TO 304
37700 TSS=TS(J)+DT*XKTS(2) /2.
37800 MJ=MJ+1
37900 GO TO 319
38000 304 CONTINUE
38100 TSS = TS(J) + DT* XKIS(3)
38200 319 CONTINUE
38300 XKIS(LJ)=RNK(J)*(T(J)-TSS) +B3*YFI*O*RO(J)*YFS(J)/EXP(E3/TSS)
38400 1 +B4*YFI*O2*RO(J)*YCS(J)/EXP(E4/TSS)
38500 320 CONTINUE
38600 TS(J) =TS(J) +DT*(XKTS(1)/6.+XKTS(2)/3.+XKTS(3)/3.+XKTS(4)/6.)
38700 YFS(J) = YF(J) /((1.+B3*RO(J)/XLE123/RNK(J))/EXP(E3/TS(J)))
38800 YCS(J) = YC(J) /((1.+B4*RO(J)/XLE223/RNK(J))/EXP(E4/TS(J)))
38900 301 CONTINUE
39000 C
39100 C END OF ONE TIME INTEGRATION STEP
39200 C *****
39300 C *****
39400 C LOOP FOR MARCHING FORWARD IN TIME
39500 C
39600 C
39700 KOUNT = KOUNT+1
39800 KOU = KOUNT-1
39900 XKOUNT = KOUNT
40000 TIME=(XKOUNT-1.)*DT
40100 IF (TIME.GT. TMAX) GC TO 999
40200 IF (MOD(KOU,IPRINT).NE.0) GO TO 200

```

```

40300      WRITE(6,22) TIME ,KCOUNT
40400      WRITE (6,13)
40500      WRITE(6,24) (T (I),I=1,NPNAS,IT)
40600      WRITE (6,9)
40700      WRITE(6,24) (TS (I), I=1,N,IT)
40800      WRITE(6,14)
40900      WRITE(6,24) (YF(I),I=1,NPNAS,IT)
41000      WRITE(6,41)
41100      WRITE(6,24) (YC(I),I=1,NPNAS,IT)
41200      WRITE(6,11)
41300      WRITE(6,24) (YFS(I),I=1,N,IT)
41400      WRITE(6,42)
41500      WRITE(6,24) (YCS(I),I=1,N,IT)
41600      WRITE(6,26)
41700      WRITE(6,24) (XJH(I),I=1,N,IT)
41800      WRITE(6,73)
41900      WRITE(6,24) (EFF(I),I=1,NPNAS,IT)
42000      WRITE(6,74)
42100      WRITE(6,24) (EFFT(I),I=1,NPNAS,IT)
42200      WRITE(6,23)
42300      GO TO 200
42400
42500      C
42600      C   END OF WHOLE INTEGRATION LOOP
42700      C   *****
42800
42900      601 CONTINUE
43000      WRITE (6,404)
43100      WRITE(6,405)
43200      999 CONTINUE
43300      STCP
      END

```

```
100      BLOCK DATA
200
300      DIMENSION TS(300),YFS(300),YCS(300)
400      COMMON /ACT1/ES1,ES2,ES3,ES4
600      COMMON /MDLEG/ WHC, WCC, WC2, WH2C
700      COMMON /TH1/XN, XM, Q1S, Q2S
800      COMMON /TH2/ CP, GC, XPR
900      COMMON /UPST/ YCI, YOI
1100     COMMON /INI/TS,YFS,YCS
1200
1400     DATA ES1,ES2,ES3,ES4/24000.,40000.,10000.,17800./
1500     DATA WHC,WC0,WC2,WH2C/44.,28.,32.,18./
1600     DATA XN,XM,Q1S,Q2S/3.,8.,6491000.,2415000./
1700     DATA CP,GC,XPR/25.,2.8312E-3,0.7/
1800     DATA YCI,YOI/0.,0.23/
2000     DATA TS,YFS,YCS/300*1.,300*0.,300*0./
2100     END
```


Example calculation:

```
$ RUN IGNITION.EXE:10
.18
1000.
3.
10.
.1
.0016
2.
.01
.01
1.001
20
46
80
1.5E5 0.71E14 2.5E3 1.E5
5
```

read-in data

```
φ
TI
XPI
UIUS
XLS
DS
AOAS
DX
DT
TMAX
IPRINT
N
NAS
C1, C2, C3, C4
IT
```

NO. OF GRID POINT = 46 80

TMAX = 1.00100005

YD(UPST,INI) = 0.230000 YF(UPST,INI) = 0.0113888 EQUI RATIO = 0.18000
0007

APPROACH VEL = 10.0000

CHANNEL VEL (I.U.) = 15.00000

Q1= 22.7754402 Q2= 8.4736843 DX= 0.0100000 DT= 0.0100000

TI, PR, REY, AD2UL, ADAS = 1000.00000 0.70000 408.31238 0.13797 2.00000

ADIABATIC FLAME TEMP = 1.443622

ADIAE FLAME TEMP (K) = 1443.62195

ES,S= 0.24000000E+05 0.40000000E+05 0.10000000E+05 0.17800000E+05

E,S = 12.078510 20.130850 5.032712 8.958228

C,S = 0.1500000000E+06 0.7100000371E+14 0.2500000000E+04 0.1000000000E+06

GC, XLEW1, XLEW2, XLS, DS = 0.002831 1.217766 1.526551 0.100000 0.001600

POI, XKI, CP, ALPHA = 1.059621 0.016000 285.000000 0.52982E-04

XPI = 3.00000

L/U = 0.0066667

B1S, B2S, = 0.36601332E+05 0.34534906E+09

B1, B2, B3, B4 = 0.20219805E+05 0.19078240E+09 0.46881531E+03 0.29468391E+05

INITIAL CONDITIONS (TS)

0.10000E+01 0.10000E+01 0.10000E+01 0.10000E+01 0.10000E+01 0.10000E+01 0.10000E+01
+01 0.10000E+01 0.10000E+01 0.10000E+01

INITIAL CONDITIONS (YFS)

0.00000E+00 0.00000E+00 0.00000E+00 0.00000E+00 0.00000E+00 0.00000E+00 0.00000E+00
+00 0.00000E+00 0.00000E+00 0.00000E+00

INITIAL CONDITIONS (YCS)

0.00000E+00 0.00000E+00 0.00000E+00 0.00000E+00 0.00000E+00 0.00000E+00 0.00000E+00
+00 0.00000E+00 0.00000E+00 0.00000E+00

TIME= 0.20000000 KOUNT= 21

GAS TEMPERATURE (T)

0.10000E+01 0.10279E+01 0.10351E+01 0.10393E+01 0.10420E+01 0.10437E+01 0.10447E
+01 0.10451E+01 0.10451E+01 0.10447E+01
0.10462E+01 0.10481E+01 0.10501E+01 0.10521E+01 0.10541E+01 0.10562E+01 0.10583E
+01 0.10604E+01 0.10625E+01 0.10647E+01
0.10669E+01 0.10691E+01 0.10714E+01 0.10737E+01 0.10760E+01 0.10784E+01

SOLID TEMPERATURE (TS)

0.11390E+01 0.10786E+01 0.10631E+01 0.10542E+01 0.10477E+01 0.10427E+01 0.10384E
+01 0.10349E+01 0.10321E+01 0.10295E+01

CNAM MASS FRACTION (YF)

0.10000E+01 0.82811E+00 0.72848E+00 0.64850E+00 0.58054E+00 0.52141E+00 0.46932E
+00 0.42307E+00 0.38150E+00 0.34400E+00
0.33115E+00 0.32383E+00 0.31646E+00 0.30902E+00 0.30153E+00 0.29398E+00 0.28638E
+00 0.27871E+00 0.27100E+00 0.26324E+00
0.25542E+00 0.24756E+00 0.23966E+00 0.23171E+00 0.22373E+00 0.21571E+00

YCD =

0.00000E+00 0.11484E-01 0.22136E-01 0.31487E-01 0.39522E-01 0.46303E-01 0.51923E
-01 0.56483E-01 0.60031E-01 0.62661E-01
0.73834E-01 0.87281E-01 0.10073E+00 0.11418E+00 0.12762E+00 0.14103E+00 0.15440E
+00 0.16772E+00 0.18098E+00 0.19417E+00
0.20726E+00 0.22024E+00 0.23309E+00 0.24579E+00 0.25833E+00 0.27068E+00

SURFACE HC MASS FRACTION (YFS)

0.53851E+00 0.24678E+00 0.20088E+00 0.17326E+00 0.15271E+00 0.13598E+00 0.12175E
+00 0.10985E+00 0.99795E-01 0.90590E-01

YCD(SURFACE) =

0.00000E+00 0.26429E-02 0.48789E-02 0.68753E-02 0.86412E-02 0.10176E-01 0.11484E
-01 0.12628E-01 0.13636E-01 0.14440E-01

XJH

0.11677E+02 0.32271E+01 0.26856E+01 0.24599E+01 0.23328E+01 0.22489E+01 0.21875E
+01 0.21536E+01 0.21464E+01 0.21403E+01

EFFICIENCY (CARBON-BALANCE)

0.00000E+00 0.16939E+00 0.26670E+00 0.34465E+00 0.41086E+00 0.46852E+00 0.51939E
+00 0.56464E+00 0.60544E+00 0.64237E+00
0.65279E+00 0.65718E+00 0.66163E+00 0.66614E+00 0.67071E+00 0.67534E+00 0.68004E
+00 0.68480E+00 0.68963E+00 0.69452E+00
0.69949E+00 0.70453E+00 0.70964E+00 0.71482E+00 0.72008E+00 0.72541E+00

EFFICIENCY (TEMPERATURE)

0.00000E+00 0.62838E-01 0.79086E-01 0.88607E-01 0.94669E-01 0.98477E-01 0.10066E
+00 0.10160E+00 0.10161E+00 0.10085E+00
0.10409E+00 0.10848E+00 0.11292E+00 0.11743E+00 0.12200E+00 0.12663E+00 0.13133E
+00 0.13609E+00 0.14092E+00 0.14582E+00
0.15079E+00 0.15582E+00 0.16093E+00 0.16611E+00 0.17137E+00 0.17670E+00

TIME= 0.40000001 KDUNT= 41

GAS TEMPERATURE (T)

0.10000E+01 0.10491E+01 0.10635E+01 0.10720E+01 0.10776E+01 0.10811E+01 0.10833E
+01 0.10843E+01 0.10845E+01 0.10841E+01
0.10861E+01 0.10889E+01 0.10917E+01 0.10945E+01 0.10975E+01 0.11004E+01 0.11035E
+01 0.11065E+01 0.11097E+01 0.11129E+01
0.11161E+01 0.11194E+01 0.11228E+01 0.11262E+01 0.11297E+01 0.11332E+01

SOLID TEMPERATURE (TS)

0.12213E+01 0.11518E+01 0.11246E+01 0.11083E+01 0.10964E+01 0.10869E+01 0.10789E
+01 0.10722E+01 0.10667E+01 0.10617E+01

CNHH MASS FRACTION (YF)

0.10000E+01 0.80758E+00 0.70137E+00 0.61707E+00 0.54601E+00 0.48467E+00 0.43108E
+00 0.38389E+00 0.34185E+00 0.30433E+00
0.26925E+00 0.27908E+00 0.26883E+00 0.25851E+00 0.24613E+00 0.23769E+00 0.22719E
+00 0.21666E+00 0.20609E+00 0.19550E+00
0.18489E+00 0.17429E+00 0.16370E+00 0.15314E+00 0.14264E+00 0.13221E+00

YCD =

0.00000E+00 0.13222E-01 0.26772E-01 0.39234E-01 0.50220E-01 0.59608E-01 0.67399E
-01 0.73657E-01 0.78404E-01 0.81781E-01
0.96870E-01 0.11495E+00 0.13288E+00 0.15060E+00 0.16809E+00 0.18529E+00 0.20218E
+00 0.21869E+00 0.23479E+00 0.25040E+00
0.26548E+00 0.27995E+00 0.29376E+00 0.30682E+00 0.31907E+00 0.33043E+00

SURFACE HC MASS FRACTION (YFS)

0.46424E+00 0.19836E+00 0.16474E+00 0.14380E+00 0.12762E+00 0.11403E+00 0.10218E
+00 0.92277E-01 0.83510E-01 0.75424E-01

YCD(SURFACE) =

0.00000E+00 0.20352E-02 0.42042E-02 0.63776E-02 0.84571E-02 0.10376E-01 0.12090E
-01 0.13661E-01 0.15024E-01 0.16140E-01

XJH

0.11677E+02 0.32624E+01 0.27297E+01 0.25095E+01 0.23858E+01 0.23039E+01 0.22435E
+01 0.22180E+01 0.22112E+01 0.22049E+01

EFFICIENCY (CARBON-BALANCE)

0.00000E+00 0.18954E+00 0.29281E+00 0.37440E+00 0.44306E+00 0.50236E+00 0.55425E
+00 0.60008E+00 0.64109E+00 0.67788E+00
0.68968E+00 0.69592E+00 0.70227E+00 0.70873E+00 0.71531E+00 0.72200E+00 0.72882E
+00 0.73577E+00 0.74284E+00 0.75003E+00
0.75736E+00 0.76481E+00 0.77240E+00 0.78011E+00 0.78795E+00 0.79591E+00

EFFICIENCY (TEMPERATURE)

0.00000E+00 0.11074E+00 0.14304E+00 0.16233E+00 0.17485E+00 0.18292E+00 0.18775E
+00 0.19010E+00 0.19058E+00 0.18953E+00
0.19407E+00 0.20031E+00 0.20666E+00 0.21312E+00 0.21970E+00 0.22640E+00 0.23322E
+00 0.24016E+00 0.24723E+00 0.25443E+00
0.26175E+00 0.26921E+00 0.27679E+00 0.28451E+00 0.29234E+00 0.30031E+00

TIME= 0.59999996 KDUNT= 61

GAS TEMPERATURE (T)

0.10000E+01 0.10637E+01 0.10848E+01 0.10979E+01 0.11067E+01 0.11127E+01 0.11166E+01
0.11188E+01 0.11198E+01 0.11197E+01
0.11225E+01 0.11262E+01 0.11301E+01 0.11340E+01 0.11380E+01 0.11421E+01 0.11463E+01
0.11506E+01 0.11550E+01 0.11594E+01
0.11640E+01 0.11686E+01 0.11733E+01 0.11780E+01 0.11828E+01 0.11876E+01

SOLID TEMPERATURE (TS)

0.12635E+01 0.12134E+01 0.11791E+01 0.11578E+01 0.11419E+01 0.11289E+01 0.11179E+01
0.11088E+01 0.11011E+01 0.10940E+01

CNHM MASS FRACTION (YF)

0.10000E+01 0.79629E+00 0.68495E+00 0.59669E+00 0.52239E+00 0.45843E+00 0.40278E+00
0.35401E+00 0.31086E+00 0.27270E+00
0.25498E+00 0.24161E+00 0.22817E+00 0.21469E+00 0.20118E+00 0.18767E+00 0.17418E+00
0.16074E+00 0.14739E+00 0.13416E+00
0.12109E+00 0.10825E+00 0.95689E-01 0.83472E-01 0.71677E-01 0.60388E-01

YCO =

0.00000E+00 0.14469E-01 0.30578E-01 0.46066E-01 0.60086E-01 0.72238E-01 0.82367E-01
0.90438E-01 0.96435E-01 0.10054E+00
0.11961E+00 0.14221E+00 0.16422E+00 0.18553E+00 0.20602E+00 0.22560E+00 0.24413E+00
0.26148E+00 0.27750E+00 0.29206E+00
0.30499E+00 0.31614E+00 0.32534E+00 0.33244E+00 0.33728E+00 0.33972E+00

SURFACE HC MASS FRACTION (YFS)

0.43022E+00 0.16752E+00 0.14035E+00 0.12323E+00 0.10966E+00 0.97974E-01 0.87588E-01
0.78891E-01 0.70921E-01 0.63536E-01

YCO(SURFACE) =

0.00000E+00 0.16102E-02 0.35915E-02 0.57604E-02 0.79705E-02 0.10111E-01 0.12099E-01
0.13980E-01 0.15616E-01 0.16983E-01

XJH

0.11677E+02 0.32865E+01 0.27628E+01 0.25486E+01 0.24291E+01 0.23501E+01 0.22915E+01
0.22746E+01 0.22690E+01 0.22633E+01

EFFICIENCY (CARBON-BALANCE)

0.00000E+00 0.20056E+00 0.30840E+00 0.39329E+00 0.46453E+00 0.52586E+00 0.57930E+00
0.62632E+00 0.66817E+00 0.70543E+00
0.71900E+00 0.72746E+00 0.73610E+00 0.74495E+00 0.75400E+00 0.76325E+00 0.77271E+00
0.78238E+00 0.79225E+00 0.80231E+00
0.81256E+00 0.82298E+00 0.83354E+00 0.84421E+00 0.85495E+00 0.86571E+00

EFFICIENCY (TEMPERATURE)

0.00000E+00 0.14356E+00 0.19111E+00 0.22064E+00 0.24056E+00 0.25404E+00 0.26275E+00
0.26777E+00 0.26994E+00 0.26975E+00
0.27609E+00 0.28455E+00 0.29320E+00 0.30204E+00 0.31109E+00 0.32034E+00 0.32980E+00
0.33947E+00 0.34934E+00 0.35940E+00
0.36965E+00 0.38007E+00 0.39063E+00 0.40130E+00 0.41204E+00 0.42280E+00

TIME= 0.80000001 KDUNT= 81

GAS TEMPERATURE (T)

0.10000E+01 0.10736E+01 0.11008E+01 0.11183E+01 0.11306E+01 0.11392E+01 0.11452E
+01 0.11490E+01 0.11512E+01 0.11519E+01
0.11557E+01 0.11606E+01 0.11656E+01 0.11708E+01 0.11761E+01 0.11816E+01 0.11871E
+01 0.11928E+01 0.11986E+01 0.12045E+01
0.12104E+01 0.12162E+01 0.12220E+01 0.12276E+01 0.12330E+01 0.12380E+01

SOLID TEMPERATURE (TS)

0.12842E+01 0.12637E+01 0.12263E+01 0.12021E+01 0.11836E+01 0.11683E+01 0.11551E
+01 0.11442E+01 0.11347E+01 0.11258E+01

CNHM MASS FRACTION (YF)

0.10000E+01 0.78985E+00 0.67457E+00 0.58286E+00 0.50547E+00 0.43878E+00 0.38082E
+00 0.33013E+00 0.28551E+00 0.24636E+00
0.22574E+00 0.20896E+00 0.19220E+00 0.17549E+00 0.15888E+00 0.14244E+00 0.12625E
+00 0.11038E+00 0.94950E-01 0.80069E-01
0.65879E-01 0.52539E-01 0.40228E-01 0.29146E-01 0.19511E-01 0.11553E-01

YCD =

0.00000E+00 0.15324E-01 0.33574E-01 0.51842E-01 0.68808E-01 0.83726E-01 0.96218E
-01 0.10609E+00 0.11328E+00 0.11798E+00
0.14070E+00 0.16711E+00 0.19204E+00 0.21529E+00 0.23659E+00 0.25571E+00 0.27238E
+00 0.28632E+00 0.29728E+00 0.30498E+00
0.30918E+00 0.30970E+00 0.30638E+00 0.29913E+00 0.28799E+00 0.27306E+00

SURFACE HC MASS FRACTION (YFS)

0.41453E+00 0.14723E+00 0.12338E+00 0.10845E+00 0.96428E-01 0.85904E-01 0.76418E
-01 0.68448E-01 0.60959E-01 0.54005E-01

YCD(SURFACE) =

0.00000E+00 0.13253E-02 0.30987E-02 0.51695E-02 0.73836E-02 0.96090E-02 0.11737E
-01 0.13799E-01 0.15599E-01 0.17119E-01

XJH

0.11677E+02 0.33030E+01 0.27876E+01 0.25795E+01 0.24646E+01 0.23889E+01 0.23328E
+01 0.23243E+01 0.23206E+01 0.23162E+01

EFFICIENCY (CARBON-BALANCE)

0.00000E+00 0.20682E+00 0.31813E+00 0.40586E+00 0.47956E+00 0.54301E+00 0.59825E
+00 0.64679E+00 0.68985E+00 0.72798E+00
0.74366E+00 0.75469E+00 0.76603E+00 0.77768E+00 0.78965E+00 0.80193E+00 0.81450E
+00 0.82733E+00 0.84038E+00 0.85359E+00
0.86686E+00 0.88009E+00 0.89312E+00 0.90578E+00 0.91784E+00 0.92905E+00

EFFICIENCY (TEMPERATURE)

0.00000E+00 0.16600E+00 0.22721E+00 0.26670E+00 0.29434E+00 0.31389E+00 0.32731E
+00 0.33593E+00 0.34078E+00 0.34242E+00
0.35100E+00 0.36203E+00 0.37337E+00 0.38503E+00 0.39700E+00 0.40928E+00 0.42185E
+00 0.43468E+00 0.44773E+00 0.46093E+00
0.47421E+00 0.48744E+00 0.50047E+00 0.51313E+00 0.52519E+00 0.53639E+00

TIME= 1.00000000 KDUNT= 101

GAS TEMPERATURE (T)

0.10000E+01 0.10805E+01 0.11129E+01 0.11345E+01 0.11501E+01 0.11616E+01 0.11698E
+01 0.11755E+01 0.11792E+01 0.11811E+01
0.11861E+01 0.11922E+01 0.11986E+01 0.12052E+01 0.12120E+01 0.12189E+01 0.12259E
+01 0.12330E+01 0.12401E+01 0.12470E+01
0.12536E+01 0.12597E+01 0.12651E+01 0.12696E+01 0.12730E+01 0.12757E+01

SOLID TEMPERATURE (TS)

0.12942E+01 0.13041E+01 0.12666E+01 0.12412E+01 0.12213E+01 0.12045E+01 0.11899E
+01 0.11778E+01 0.11670E+01 0.11568E+01

CNRM MASS FRACTION (YF)

0.10000E+01 0.78602E+00 0.66774E+00 0.57313E+00 0.49291E+00 0.42358E+00 0.36325E
+00 0.31050E+00 0.26422E+00 0.22386E+00
0.20022E+00 0.18001E+00 0.15997E+00 0.14021E+00 0.12085E+00 0.10205E+00 0.83997E
-01 0.66901E-01 0.51025E-01 0.36667E-01
0.24163E-01 0.13877E-01 0.61870E-02 0.14578E-02 0.00000E+00 0.00000E+00

YCD =

0.00000E+00 0.15904E-01 0.35886E-01 0.56611E-01 0.76315E-01 0.93878E-01 0.10864E
+00 0.12020E+00 0.12840E+00 0.13347E+00
0.15912E+00 0.18804E+00 0.21403E+00 0.23668E+00 0.25556E+00 0.27025E+00 0.28033E
+00 0.28546E+00 0.28534E+00 0.27984E+00
0.26894E+00 0.25285E+00 0.23195E+00 0.20684E+00 0.17831E+00 0.15073E+00

SURFACE HC MASS FRACTION (YFS)

0.40722E+00 0.13348E+00 0.11127E+00 0.97579E-01 0.86488E-01 0.76671E-01 0.67731E
-01 0.60191E-01 0.52984E-01 0.46285E-01

YCD(SURFACE) =

0.00000E+00 0.11340E-02 0.27210E-02 0.46606E-02 0.68086E-02 0.90267E-02 0.11191E
-01 0.13321E-01 0.15180E-01 0.16751E-01

XJH

0.11677E+02 0.33143E+01 0.28063E+01 0.26039E+01 0.24936E+01 0.24215E+01 0.23683E
+01 0.23678E+01 0.23657E+01 0.23641E+01

EFFICIENCY(CARBON-BALANCE)

0.00000E+00 0.21052E+00 0.32445E+00 0.41456E+00 0.49049E+00 0.55600E+00 0.61311E
+00 0.66335E+00 0.70785E+00 0.74710E+00
0.76517E+00 0.77909E+00 0.79347E+00 0.80830E+00 0.82355E+00 0.83916E+00 0.85502E
+00 0.87100E+00 0.88690E+00 0.90246E+00
0.91733E+00 0.93112E+00 0.94335E+00 0.95355E+00 0.96121E+00 0.96721E+00

EFFICIENCY(TEMPERATURE)

0.00000E+00 0.18145E+00 0.25441E+00 0.30314E+00 0.33837E+00 0.36422E+00 0.38283E
+00 0.39570E+00 0.40395E+00 0.40818E+00
0.41940E+00 0.43332E+00 0.44770E+00 0.46253E+00 0.47778E+00 0.49339E+00 0.50925E
+00 0.52523E+00 0.54113E+00 0.55669E+00
0.57156E+00 0.58535E+00 0.59758E+00 0.60778E+00 0.61546E+00 0.62146E+00

APPENDIX II

LISTING OF COMPUTER PROGRAMS FOR CHAPTER II

The computer programs for Part II (steady state) are quite similar, in structure, to those in Part I. In addition to using a three-reactions scheme as discussed in the text of Part II, only the final results are printed out (no intermediate transient).

More Detailed Instruction (for CALY1. FOR; 75):

1. Read-in data (lines 10400 - 11475):

XPHI = ϕ = fuel-air equivalence ratio

TI = T(0,0) = upstream, initial temperature (K)

XPI = $p(0,0)$ = upstream, initial pressure (Atm.)

UIUS = U_{ref} = upstream (outside of the bed) initial gas velocity (m/s)

XLS = reference length (m), suggested to use 0.1m (10 cm)

DS = d^* = channel hydraulic diameter (m)

AOAS = A^*/A_s^* = open-to-close area ratio

DXX = nondimensional step size in X (space) inside the catalytic bed. It is nondimensionalized by XLS. So if XLS = 0.1 m and DX = 0.01, the dimensional step size is 0.001 m or 1mm.

XAS = ratio of step sizes between downstream and inside-bed regions. For example, (XAS) x (DXX) is the integration step size in X - direction in the downstream space.

DT = nondimensional time step size, recommended to be 0.2 or 0.1 for steady calculations.

TMAX = maximum nondimensional time allowed for computation.

It should be large enough to allow the steady state to be reached. For bed length less than 5 cm, TMAX = 8.001 is suggested, for bed length between 5 - 12 cm, TMAX = 12.001 is suggested.

N = number of grid points (in X direction) in the catalytic bed. The nondimensional catalytic bed length is given by $(N-1) \times (DX)$. For example, if $N = 51$, $DX = .01$, then the nondimensional bed length is equal to 0.5. If $XLS = .1m$, then the dimensional bed length is .05m (5 cm).

NAS = number of grid points (in X - direction) in the downstream after-bed space. The length of the downstream distance can be calculated in a similar manner as in the above.

IT = interval in X for printout. For example, if $DXX = .01$, $IT = 5$, the printout will be at $X = 0, 0.05, 0.1, 0.15,$ etc. ...

CO, C1, C2, C3, C4 = C_1, C_2, C_3, C_4 (See Table I)

IPUTIN = 1 (always)

2. Output data (lines 37000 -38586):

The following quantities will be printed out as a function of downstream distance:

Gas and solid temperatures, Emission indices (x1000) for the original hydrocarbon, pyrolyzed hydrocarbon, total hydrocarbon and CO in the gas phase, the original hydrocarbon and CO at the wall and the combustion efficiency.

If TMAX is large enough, the above printouts are the steady-state profiles.

```

100
200 *****
300 *** STEADY CATALYTIC COMBUSTOR ***
400 *****
500
525 THREE GAS-PHASE REACTION STEPS
537
550 VARIABLE X STEFF SIZE ( BED VS. AFTER-BED SPACE )
575
600 PARAMETER NX=300
800 COMMON /ACTI/ ESO,ES1,ES2,ES3,ES4
900 COMMON /MOLEQ/ WHC, WCC, WC2, WH2O
1000 COMMON /TH1/XN, XM, Q1S, Q2S
1100 COMMON /TH2/ CP, GC, XPR
1200 COMMON /UPST/ YCI, YOI
1400 COMMON /INI/ IS, YFS, YCS, YES
1450 COMMON /B12345/ B1A1, B1A2, B1A3, B1A4, B1A5
1475 COMMON /GAMMA/ GAMA
1500
1600 DIMENSION YF(NX), T(NX), TS(NX), YO(NX), YFS(NX), KC(NX), U(NX)
1700 DIMENSION XKY(4), XKT(4), XKIS(4), XKC(4), YC(NX), YCS(NX)
1800 DIMENSION XJH(NX), XJD1(NX), XJD2(NX), YH2O(NX), XP(NX)
1850 DIMENSION EFF(NX), RNK(NX)
1875 DIMENSION A(NX,3), XKE(4), YE(NX), YTHC(NX), YES(NX)
1887 EQUIVALENC ( A(1,1),TS(1), ( A(1,2),YFS(1)), ( A(1,3),YCS(1))
1900
2000 7 FORMAT (4E20.10)
2100 8 FORMAT (I4)
2200 9 FORMAT (1H0,'SOLID TEMPERATURE (TS)'/)
2300 10 FORMAT (6F12.6)
2400 11 FORMAT (1H0,'SURFACE HC MASS FRACTION (YFS)'/)
2500 12 FORMAT (//)
2600 13 FORMAT (1H0,'GAS TEMPERATURE (T)'/)
2700 14 FORMAT (1H0,'ORIGINAL CNHM (YF)'/)
2800 15 FORMAT (1H0,'YG(UPST,INI) =',F10.6,5X,'YF (UPST,INI) =',F10.7,
2900 1 SX,'EQUI RATIC =',F15.9//)
3000 17 FORMAT (1H0,'O1=',F15.7,5X,'O2=',F15.7,5X,'Ox=',F15.7,5X,'DT=',
3100 1F15.7//)
3200 18 FORMAT (1H0,'N=',I10//)
3300 19 FORMAT (1H0,'INITIAL CONDITIONS (TS)',/)
3400 20 FORMAT (1H0,'TMAX =',F15.8)
3500 21 FORMAT (1H0,'NO. OF GRID POINT =',I21//)
3600 22 FORMAT (1H0,'TIME =',F15.8,5X,'KOUNT =',I10//)
3700 23 FORMAT (///)
3800 24 FORMAT (10E12.5)
3900 25 FORMAT (1H0,'INITIAL CONDITIONS (YFS)',/)
4000 26 FORMAT (1H0,'XJH'//)
4100 31 FORMAT (1H0,'CC MASS FRACTION (YC)'/)
4200 32 FORMAT (1H0,'SURFACE CO MASS FRACTION (YCS)'/)
4300 33 FORMAT (1H0,'INITIAL CONDITIONS (YCS)',/)
4400 34 FORMAT (1H0,' ES,S =',6F12.6//)
4500 35 FORMAT (1H0,' C,S =',5E20.10//)
4600 36 FORMAT (1H0,' A,S =',6F12.6//)
4700 37 FORMAT (1H0,' BE,S =',6F12.6//)
4800 41 FORMAT (1H0,' YCC =',/)
4900 42 FORMAT (1H0,' YCC(SURFACE) =',/)
5000 43 FORMAT (1H0,' L/U =',F15.7//)
5100 44 FORMAT (1H0,' B1S, B2S =',4E15.8//)
5200 45 FORMAT (1H0,' B0-4 =',5E15.8//)
5300 46 FORMAT (4E20.8)
5400 47 FORMAT (1H0,' E,S =',6F12.6//)
5500 48 FORMAT (1H0,' GC, XLEW1, XLEW2, XLS, DS =',6F12.6//)
5600 49 FORMAT (1H0,' ROI, XKI, CP, ALPHA =',3F12.6,E12.5//)
5700 71 FORMAT (1H0,' APPROACH VEL =',F10.4//)
5800 72 FORMAT (1H0,' CHANNEL VEL (I.U.) =',F10.5//)
5850 73 FORMAT (1H0,' EFFICIENCY(CARBON-BALANCE)',/)
5900 401 FORMAT (1H0,' XPI =',F20.5//)
6000 402 FORMAT (1H0,' TI, PR, REY, AD2UL, AGAS =',5F12.5//)
6100 403 FORMAT (1H0,' ES,S =',5E20.8//)
6200 404 FORMAT (1H0,' *****',/)
6300 405 FORMAT (1H0,' GAS TEMPERATURE IS NEGATIVE')
6400 406 FORMAT (1H0,' CNHM CONCENTRATICN IS NEGATIVE')
6500 407 FORMAT (1H0,' CC CONCENTRATICN IS NEGATIVE')
6600 408 FORMAT (1H0,' YFF IS NEGATIVE')
6650 409 FORMAT (1H0,' ADIABATIC FLAME TEMP =',F10.6//)
6675 410 FORMAT (1H0,' ADIAE FLAME TEMP(K) =',F15.5//)
6687 411 FORMAT (1H0,' BETA 1-5 =',5F10.4//)
6743 412 FORMAT (1H0,' PYRGLYZED CNHM (YE)',/)
6799 413 FORMAT (1H0,' TOTAL CNHM (YTHC)',/)
6800 *****
6900

```

```

7000      ***** INPUT PARAMETERS      *****
7100
7200      ***** CHEMICAL PARAMETERS      *****
7300
7400
7450      CHEMICAL REACTION 0,  CNHM = CNHM (GAS PHASE PYROLYSIS)
7475      (ISOTHERMAL REACTION)
7500      CHEMICAL REACTION 1,  CNHM + O2 = CO +H2O (GAS PHASE)
7600      CHEMICAL REACTION 2,  CO + O2 = CO2 (GAS PHASE)
7700      CHEMICAL REACTION 3,  CNHM +O2 = CO2 + H2O ( SOLID SURFACE)
7800      CHEMICAL REACTION 4,  CO + O2 = CO2 (SOLID SURFACE)
7900
8000
8100      ES1 = ACTIVATION ENERGY FOR REACTION 1 (CAL/MOLE), ETC.
8200      C1 = PREEXPONENTIAL FACTOR (DIMENSIONAL) FOR REACTION 1, ETC.
8300      WHC, WCO = MOLECULAR WEIGHTS FOR CNHM, CO
8400      Q1S = HEAT OF COMBUSTION FOR REACTION 1 (CAL/G OF CNHM)
8500      Q2S = HEAT OF COMBUSTION FOR REACTION 2 (CAL/G OF CO)
8600      QS = HEAT OF COMBUSTION FOR REACTION 3 ( CAL/G OF CNHM)
8700      XN = THE NUMBER OF CARBONS IN CNHM
8800      XM = THE NUMBER OF HYDROGEN IN CNHM
8900
9000
9100
9200      QS = Q1S + Q2S*XN*WCO/WHC
9300
9400      ***** CATALYTIC BED PARAMETERS      *****
9500
9600      XLS = BED LENGTH (M)
9700      DS = CHANNEL HYDRAULIC DIAMETER(M)
9800      SOA = CIRCUMFERENTIAL LENGTH DIVIDED BY CHANNEL AREA,=4/DS (1/M)
9900      AOAS = RATIO OF OPEN TO CLOSED AREAS
10000     CSS = HEAT CAPACITY OF SUBSTRATE (CAL/KG/K)
10100     ROS= DENSITY OF SUBSTRATE (KG/ M3)
10200
10300
10400     READ(5,10) XPHI
10500     READ (5,10) TI
10600     READ (5,10) XPI
10700     READ (5,10) UIUS
10800     READ (5,10) XLS
10900     READ (5,10) DS
11000     READ (5,10) AOAS
11100     READ(5,*) DXX, XAS
11200     READ (5,10) DT
11300     READ (5,10) TMAX
11400     READ(5,8) N
11425     READ(5,8) NAS
11437     READ(5,8) IT
11450     READ(5,*) CO,C1,C2,C3,C4
11475     READ(5,8) IPUTIN
11500     SOA = 4.0/DS
11600     CN = XN*WCO/WHC
11650     NPNAS=N+NAS
11700
11800     ***** OPERATING PARAMETERS      *****
11900     TI = INITIAL, UPSTREAM (I.U.) TEMPERATURE (K)
12000     UI = I.U. VELOCITY (M/S)
12100     XPI = I. U. PRESSURE (ATM.)
12200     ROI= I.U. GAS DENSITY (KG/M3)
12300     YFI = I.U. MASS FRACTION OF HC
12400     YCI = I.U. MASS FRACTION OF CC
12500     YOI = I.U. MASS FRACTION OF O2
12600     XPHI = UPSTREAM HC/O2 EQUIVALENCE RATIO
12700
12800
12900     UI = UIUS*(1.0+AOAS)/AOAS
13000     XNU = 0.000001458*SQRT(TI)/(1.0+110.4/TI)
13100     YFI=WHC*XPHI/29./((XN+XM/4.)*4.76+XPHI)
13200     XLEW1 = 1.5* SQRT (29./WHC)
13300     XLEW2=1.5* SQRT(29./WCO)
13350     XLE123=XLEW1**.667
13375     XLE223=XLEW2**.667
13400
13500     XLOU = XLS/UI
13600
13700     ***** GAS PROPERTY      *****
13800
13900
14000     CP = SPECIFIC HEAT OF GAS (CAL/KG/K)
14100     XKI = HEAT CONDUCTIVITY OF GAS AT I.U. (CAL/ M/SEC/K)

```

```

14200 ALPHA = 1.0, GAS THERMAL DIFFUSIVITY ( M2/SEC)
14300 GC=GAS CONSTANT FOR GAS MIXTURE (J/CM3/KG/K)
14400 XLEW1 = LEWIS NUMBER FOR CNHM IN MIXTURE
14500 XLEW2 = LEWIS NUMBER FOR CO IN MIXTURE
14600
14700
14750 XKI=.003+.000013*TI
14800 ROI = XPI/GC/TI
14900 ALPHA = XKI/RCI/CP
15000 REY = UIUS*DS*RCI/XMU
15100
15200
15300 TO DESCRIBE CHEMICAL REACTION RATE EXPRESSIONS
15350 REACTION 0 (GAS PHASE ISOTHERMAL PYROLYSIS)
15375 D(CNHM)/DT $$$ (CNHM)/EXP(E0/RT)
15387
15400 REACTION 1 ( GAS PHASE )
15500 D(CNHM)/DT $$$ XP**.3*TI*SQRT(YHC)*Y02/EXP(E1/RT)
15600
15700 REACTION 2 (GAS PHASE )
15800 D(CO)/DT $ P**BIA1*CO**BTA2*O2**BTA3*TI**BTA4*H2O**PTA5/EXP(E2/RT)
15900
16000 REACTION 3 (SOLID SURFACE)
16100 D(CNHM)/DT $$$ YHCS/EXP(E3/RT)
16200
16300 REACTION 4 (SOLID SURFACE)
16400 D(CC)/DT $$$ YCCS/EXP(E4/RT)
16500
16600 TO EVALUATE KINETIC RATE CONSTANTS.
16700
16750 B0=CO*XLOU*(WHC/ROI/YFI)**(1.-GAMA)
16800 B1SS = C1*SQRT(WPC)/WC2/SQRT(1000.)
16900 B1S = B1SS*XPI**.3*RCI*SQRT(RCI)*TI*SQRT(YFI)*Y01
17000 B1 = XLOU*B1S/RCI/YFI
17100 B235=BTA2+BTA3+BTA5
17150 C2M=C2*1000.**((1.-B235)
17200 B2SS=C2M*WC**((1.-BTA2)/(WC2**BTA3*H2O**BTA5)
17300 B2S=B2SS*XPI**BTA1*ROI**B235*TI**BTA4*YFI**BTA2*Y01**BTA3
17400 B2 = B2S*XLOU/RCI/YFI
17500
17900 B3=C3*DS/ALPHA/WC/3.66
17950 B4=C4*DS/ALPHA/WCO/3.66
18000 Q1 = Q1S/CP/TI
18100 Q2 = Q2S/CP/TI
18200 Q = QS/CP/TI
18250 TAB=YF1*U+1.0
18275 TABDM=TAB*TI
18287 E0= ES0/TI/1.987
18300 E1= ES1/TI/1.987
18400 E2= ES2/TI/1.987
18500 E3= ES3/TI/1.987
18600 E4= ES4/TI/1.987
18700 AD2UL = (ALPHA/DS/DS) / (UI/XLS)
18800 *****
18900
19000 WRITE (6,21) N,NAS
19100 WRITE(6,20) TMAX
19200 WRITE (6,15) YCI, YFI, XPHI
19300 WRITE(6,71) UIUS
19400 WRITE (6,72) UI
19500 WRITE (6,17) Q1, Q2, DXX, DI
19600 WRITE (6,402)TI,XPR,REY, AD2UL, ADAS
19650 WRITE(6,409) TAB
19675 WRITE(6,410) TABDM
19700 WRITE (6,403)ES0,ES1,ES2,ES3,ES4
19800 WRITE(6,47)E0,E1,E2,E3,E4
19900 WRITE(6,35)C0,C1,C2,C3,C4
19950 WRITE (6,411) BTA1,BTA2,BTA3,BTA4,BTA5
20000 WRITE (6,48) GC, XLEW1, XLEW2, XLS, DS
20100 WRITE (6,49) ROI, XKI, CP, ALPHA
20200 WRITE (6,401) XPI
20300 WRITE (6,43) XLCU
20400 WRITE (6,44) B1S, B2S
20500 WRITE(6,45)B0,B1,B2,B3,P4
21100
21200
21300 *****
21400
21500 ***** UPSTREAM CONDITIONS
21600 YF(1)=1.
21650 YE(1)=0.

```

```

21700      YC(1) = 0.0
21800      YC(1)=1.
21900      T(1)=1.
22000      RO(1)=1.
22100      XP(1)=1.0
22200      U(1)=1.
22250      YTHC(1) = YF(1)+YE(1)
22300
22400      *****
23000
23100      *****
23200      START OF INTEGRATION LCOF
23300      KOUNT = 1
23350      XNUO=.885*SQRT(ACAS)*SQRT(XPR*REY)
23375      ROOT1=0.0
23387      ROOT2=1.0
23393      555      ROOT=.5*(ROOT1+RCOT2)
23396      IF(RCOT.LE.0.1) YNU=.0444/ROCI+3.46-1.34*RCOT
23397      IF(RCOT.GT.0.1) YNU=0.011/ROOT+3.66
23398      YROCI=YNU-XNUO
23449      IF(ABS(YROOT).LJ.0.01) GO TO 200
23474      IF(YROOT.GT.0.0) ROOT1=ROOT
23487      IF(YROOT.LE.0.0) ROOT2=ROOT
23493      GO TO 555
23500      200      CONTINUE
23550      DMASS=RO(1)*U(1)
23600
23700      INTEGRATION OF QUASI-STEADY GAS PHASE EQUATIONS FOR
23800      YF (FUEL MASS FRACTION) AND T (TEMPERATURE) IN DOWNSTREAM
23900      DIRECTION USING FOURTH-ORDER RUNGE-KUTTA SCHEME
24000      I IS THE INDEX FOR DOWNSTREAM DISTANCE X
24100
24200
24300      DO 201 I=1,NPNAS
24350
24362      IF(I.LE.N) DX=DXX
24374      IF(I.GT.N) DX=XAS*DXX
24375      IF(I.GT.N)DMASS=RO(1)*U(1)*ACAS/(ACAS+1.)
24400      *****
24500
24600      EVALUATE XJH AND XJD AS A FUNCTION OF X
24700
24800      *****
24900      NONDIMENSIONAL HEAT CONDUCTIVITY
25000      XK = (.003+ 0.000013* T1 *I(I)) /XK1
25100      *****
25200
25300      IF(I.GT.1) GO TO 180
25325      IF(I.EQ.1) X=0.0
25337      GO TO 181
25349      180      CONTINUE
25350      IX=I+1
25450      XI=IX-1
25500      X = XI*DX
25550      181      CONTINUE
25600      XST= X*2.0*AD2UL*XK+ROCI
25700      IF(XST.LE.0.1) XNU=0.0444/XST+3.46 -1.34*XST
25800      IF(XST.GT.0.1) XNU=0.011/XST +3.66
26250      RNK(I)=XNU*XK/3.66
26300      XJH(I) = 4.0*XNU *AD2UL*XK
26350      IF(I.GT.N) XJH(I) =0.0
26400      XJD1(I) = XJH(I) *XLE123
26500      XJD2(I) = XJH(I) *XLE223
26600      *****
26700
26800      132      CONTINUE
26900      M=1
27000      DO 120 L=1,4
27100      IF (M.NE.1) GO TO 102
27200      YFF= YF(I)
27250      YEE =YE(I)
27300      YCC =YC(I)
27400      TT = T(I)
27500      M=M+1
27600      GO TO 119
27700      102      CONTINUE
27800      IF (M.NE.2) GO TO 103
27900      YFF=YF(I)+DX*XKY(1) /2.
27950      YEE=YE(I)+DX*XKE(1)/2.
28000      YCC =YC(I) +DX*XKC(1)/2.
28100      TT =T(I)+DX*XKT(1) /2.

```

```

28200      M=M+1
28300      GO TC 119
28400 103 CONTINUE
28500      IF (M.NE.3) GO TC 104
28600      YFF = YF(1) + DX*XKY(2) /2.
28650      YEL = YE(I) + DX*XKE(2) /2.
28700      YCC = YC(I) + DX*XKC(2) /2.
28800      TT = T(I) + DX*XKT(2) /2.
28900      M=M+1
29000      GO TC 119
29100 104 CONTINUE
29200      YFF = YF(1) + DX*XKY(3)
29250      YEL = YE(I) + DX*XKE(3)
29300      YCC = YC(I) + DX*XKC(3)
29400      TT = T(I) + DX*XKT(3)
29500 119 CONTINUE
29600      YH2O = MASS FRACTION OF H2O
29700      YH2O(I) = .5*XM*WH2O*YF1 * (YTHC(1)-YTHC(I))/WHC
29800      IF (YFF.LT.0.0) YFF=0.0
29850      W0=B0*(RO(1)*YFF)**GAMA/EXP(E0/TT)
29875      IF (YEE.LT.0.0) YEE=0.0
29900      W1 = B1* XE(I)**.3*RO(1)*SQRT(RO(1))*T(I)*SQRT(YEE) *YO(I)
30000      1 /EXP(E1/TT)
30025      IF (YCC.LT.0.0) YCC=0.0
30050      SSYQ=YO(I)**BTA3
30075      RO235=RO(1)**B235
30100      W2=B2*RO235*SSYC*YCC**BTA2*YH2O(I)**B1A5*XP(I)**BTA1/EXP(L2/IT)
30200      XKY(L) = -XJD1(I) *(YFF- YFS(I))/DMASS -W0/DMASS
30250      XKE(L)=-XJD1(I)*(YEL-YES(I))/DMASS+(W0-W1)/DMASS
30300      XK(L) = -XJD2(I) *(YCC-YCS(I))/ DMASS +CN*W1/DMASS -W2/DMASS
30400      XKT(L) =-XJH(I)*(TT-TS(I))/DMASS +O1*YF1*W1/DMASS+O2*YF1*W2/DMASS
30500 120 CONTINUE
30600      YF(I+1) =YF(I) +DX*(XKY (1)/6. +XKY (2)/3. +XKY (3)/3.+XKY (4)/6.)
30700      IF (YF(I+1).LT.0.0) YF(I+1) =0.0
30750      YE(I+1)=YE(I)+DX*(XKE(1)/6.+XKE(2)/3.+XKE(3)/3.+XKE(4)/6.)
30775      IF (YE(I+1).LT.0.0) YE(I+1)=0.0
30800      YC(I+1) =YC(I) +DX*(XKC (1)/6. +XKC (2)/3. +XKC (3)/3.+XKC (4)/6.)
30900      IF (YC(I+1).LT.0.0) YC(I+1) =0.0
31000      T (I+1) =T (I) +DX*(XKI (1)/6. +XKI (2)/3. +XKI (3)/3.+XKI (4)/6.)
31100      IF (T(I+1).LT..0) GO TC 601
31125      YTHC(I+1)=YF(I+1)+YE(I+1)
31150      ADD=YC(I+1)*YF1*W02/YC1/KCC/2.
31200      YO(I+1) =1.0-XPH1*(1.0-YF(I+1))+ADD
31300      XP(I+1)=XP(I)
31400      RO(I+1)=XP(I+1) /T(I+1)
31500      U(I+1) =DMASS/T(I+1)
31550      EFF(I)=1.-YTHC(I)-YC(I)*Q2/O
31600 201 CONTINUE
31700
31800      END OF ONE RUNGE-KUTTA INTEGRATION CYCLE FOR QUASI-STEADY
31900      GAS PHASE EQUATIONS
32000      *****
32100
32200
32300      *****
32400      INTEGATION OF UNSTEADY SOLID HEAT TRANSFER EQUATION
32500      FOR TS ( SOLID TEMPAIURE ) IN TIME USING FOURTH-ORDER
32600      RUNGE-KUTTA SCHEME
32700
32800
32900
33000      DO 301 J =1,N
33100      MJ=1
33200      DO 320 LJ=1,4
33300      IF (MJ.NE.1) GO TO 302
33400      TSS =TS(J)
33500      MJ=MJ+1
33600      GO TO 319
33700 302 CONTINUE
33800      IF (MJ.NE.2) GO TO 303
33900      TSS = TS(J) + DT*XKTS(1)/2.
34000      MJ=MJ+1
34100      GO TO 319
34200 303 CONTINUE
34300      IF (MJ.NE.3) GO TO 304
34400      TSS=TS(J)+DT*XKTS(2) /2.
34500      MJ=MJ+1
34600      GO TC 319
34700 304 CONTINUE
34800      TSS = TS(J) + DT* XKTS(3)
34900 319 CONTINUE

```

```

34950      YFSES=YFS(J)+YES(J)
35000      XKTS(LJ)=RNK(J)*(T(J)-ISS) +B3*YFI*Q*RO(J)*YFSES/EXP(E3/TSS)
35100      1 +B4*YFI*Q2*RO(J)*YCS(J)/EXP(E4/TSS)
35200      320 CONTINUE
35300      TS(J) =TS(J) +DT*(XKTS(1)/6.+XKTS(2)/J.+XKTS(3)/3.+XKTS(4)/6.)
35400      YFS(J) = YF(J) / (1.+B3*RO(J)/XLE123/RNK(J)/EXP(E3/TS(J)))
35450      YES(J)=YE(J)/(1.+B3*RO(J)/XLE123/RNK(J)/EXP(E3/TS(J)))
35500      YCS(J) = YC(J) / (1.+B4*RO(J)/XLE223/RNK(J)/EXP(E4/TS(J)))
35600      301 CONTINUE
35700
35800      END OF ONE TIME INTEGRATION STEP
35900      *****
36000
36100      *****
36200      LOOP FOR MARCHING FORWARD IN TIME
36300
36400      KOUNT =KOUNT+1
36500      KOU  =KOUNT-1
36600      XKOUNT =KOUNT
36700      TIME=(XKOUNT-1.)*DT
36800      IF (TIME.GT. TMAX) GO TO 999
36900      TIME=TMAX-DT
36950      IF (TIME.LT. TIMER) GO TO 200
37000      WRITE(6,22) TIME ,KOUNT
37100      WRITE (6,13)
37200      WRITE(6,24) (T (I),I=1,NPNAS,IT)
37300      WRITE (6,9)
37400      WRITE(6,24) (TS (I),I=1,N,IT)
37500      WRITE(6,14)
37600      WRITE(6,24) (YF(I),I=1,NPNAS,IT)
37650      WRITE(6,412)
37675      WRITE(6,24) (YE(I),I=1,NPNAS,IT)
37687      WRITE(6,413)
37699      WRITE(6,24) (YTHC(I),I=1,NPNAS,IT)
37700      WRITE(6,41)
37800      WRITE(6,24) (YC(I),I=1,NPNAS,IT)
37900      WRITE(6,11)
38000      WRITE(6,24) (YFS(I),I=1,N,IT)
38100      WRITE(6,42)
38200      WRITE(6,24) (YCS(I),I=1,N,IT)
38300      WRITE(6,26)
38400      WRITE(6,24) (XJH(I),I=1,N,IT)
38500      WRITE(6,73)
38543      WRITE(6,24) (EFF(I),I=1,NPNAS,IT)
38586      WRITE(6,23)
38593      901 CONTINUE
38594      IF (IPUTIN.EG.1) GO TO 200
38596      OPEN(UNIT=11,TYPE='NEW',NAME='SOLID')
38599      WRITE (11,*) A
38624      CLOSE (UNIT=11)
38650      GO TO 200
38700
38800      END OF WHOLE INTEGRATION LOOP
38900      *****
39000
39100      601 CONTINUE
39200      WRITE (6,404)
39300      WRITE(6,405)
39400      999 CONTINUE
39500      STOP
39600      END

```

```

100      BLOCK DATA
200
300      DIMENSION TS(300),YFS(300),YCS(300),YES(300)
400      COMMON /ACTJ/ES0,ES1,ES2,ES3,ES4
500      COMMON /MOLEQ/ WHC, WCC, WQ2, WH2U
600      COMMON /IH1/XN, XM, Q1S, Q2S
700      COMMON /IH2/ CF, GC, XPR
800      COMMON /UPST/ YCI, YDI
900      COMMON /INI/TS,YFS,YCS,YES
1100     COMMON /B12345/BTA1,BTA2,BTA3,BTA4,BTA5
1175     COMMON /GAMMA/GAMA
1200
1400     DATA ES0,ES1,ES2,ES3,ES4/34000.,24000.,40000.,10000.,17800./
1500     DATA WHC,WCC,WQ2,WH2U/138.,28.,32.,18./
1600     DATA XN,XM,Q1S,Q2S/10.,18.,5357000.,2415000./
1700     DATA CF,GC,XPR/285.,2.8312E-3,0.7/
1800     DATA YCI,YDI/0.,0.23/
1900     DATA BTA1,BTA2,BTA3,BTA4,BTA5/0.,1.,0.25,0.,0.5/
1950     DATA GAMA/0.5/
2000     DATA TS,YFS,YCS,YES/300*1.,300*0.,300*0.,300*0./
2100     END

```


Example calculation:

```
$ RUN CALY1.EXE;61
.165
1000.
3.
15.
.1
.001382
13.29
.01 1.
.1
8.001
51
100
5
1.6E6 1.8E5 .54E14 1.5E4 1.E5
1
```



Read-in data

ϕ
TI
XPI
UTUS
XLS
DS
AOAS
DXX, XAS
DT
TMAX
N
NAS
IT
CO, CI, C2, C3, C4
IPUTIN

NO. OF GRID POINT = 51 100

TMAX = 8.00100040

YD (UPST,INI) = 0.230000 YF (UPST,INI) = 0.0113489 EQUI RATIO = 0.165
000007

APPROACH VEL = 15.0000

CHANNEL VEL (I.U.) = 16.12867

Q1= 18.7964916 Q2= 8.4736843 DX= 0.0100000 DT= 0.
1000000

TI, PR, REY, AD2UL, ADAS = 1000.00000 0.70000 529.01978 0.17199 13
.29000

ADIABATIC FLAME TEMP = 1.408440

ADIAB FLAME TEMP (K) = 1408.44019

ES,S= 0.34000000E+05 0.24000000E+05 0.40000000E+05 0.100000
00E+05 0.17800000E+05

E,S = 17.111223 12.078510 20.130850 5.032712 8.958228

C,S = 0.1600000000E+07 0.1800000000E+06 0.5399999886E+14 0.1500
000000E+05 0.1000000000E+06

BETA 1-5 = 0.0000 1.0000 0.2500 0.0000 0.5000

GC, XLEW1, XLEW2, XLS, DS = 0.002831 0.687624 1.526551 0.100000 0
.001382

POI, XKI, CP, ALPHA = 1.059621 0.016000 285.000000 0.52982E-04

XPI = 3.00000

L/U = 0.0062001

B1S, B2S, = 0.77647750E+05 0.26173910E+09

B0-4 = 0.10626966E+07 0.40033785E+05 0.13494798E+09 0.77466638E+03 0.25453324E+0
5

TIME= 8.00000000 KOUNT= 81

GAS TEMPERATURE (T)

0.10000E+01 0.10933E+01 0.11328E+01 0.11648E+01 0.11927E+01 0.12180E+01 0.12416E
+01 0.12640E+01 0.12855E+01 0.13063E+01
0.13262E+01 0.13387E+01 0.13506E+01 0.13629E+01 0.13739E+01 0.13806E+01 0.13853E
+01 0.13891E+01 0.13923E+01 0.13948E+01
0.13969E+01 0.13985E+01 0.13998E+01 0.14008E+01 0.14016E+01 0.14022E+01 0.14027E
+01 0.14031E+01 0.14034E+01 0.14036E+01
0.14038E+01

SOLID TEMPERATURE (TS)

0.11286E+01 0.13193E+01 0.13325E+01 0.13421E+01 0.13502E+01 0.13576E+01 0.13646E
+01 0.13713E+01 0.13779E+01 0.13842E+01
0.13901E+01

ORIGINAL CNHM (YF)

0.10000E+01 0.76186E+00 0.65814E+00 0.57097E+00 0.49212E+00 0.41866E+00 0.34867E
+00 0.28172E+00 0.21825E+00 0.15913E+00
0.10576E+00 0.65733E-01 0.33518E-01 0.10262E-01 0.16875E-03 0.00000E+00 0.00000E
+00 0.00000E+00 0.00000E+00 0.00000E+00
0.00000E+00 0.00000E+00 0.00000E+00 0.00000E+00 0.00000E+00 0.00000E+00 0.00000E
+00 0.00000E+00 0.00000E+00 0.00000E+00
0.00000E+00

HYDROLYZED CNHM (YE)

0.00000E+00 0.37022E-02 0.91331E-02 0.15642E-01 0.22801E-01 0.30127E-01 0.37036E-01
 -01 0.42908E-01 0.47042E-01 0.48627E-01
 0.46778E-01 0.44312E-01 0.36474E-01 0.22910E-01 0.59886E-02 0.00000E+00 0.00000E+00
 +00 0.00000E+00 0.00000E+00 0.00000E+00
 0.00000E+00 0.00000E+00 0.00000E+00 0.00000E+00 0.00000E+00 0.00000E+00 0.00000E+00
 +00 0.00000E+00 0.00000E+00 0.00000E+00
 0.00000E+00

TOTAL CNHM (YTHC)

0.10000E+01 0.76556E+00 0.66727E+00 0.58662E+00 0.51493E+00 0.44878E+00 0.38571E+00
 +00 0.32463E+00 0.26529E+00 0.20776E+00
 0.15254E+00 0.11004E+00 0.69992E-01 0.33172E-01 0.61574E-02 0.00000E+00 0.00000E+00
 +00 0.00000E+00 0.00000E+00 0.00000E+00
 0.00000E+00 0.00000E+00 0.00000E+00 0.00000E+00 0.00000E+00 0.00000E+00 0.00000E+00
 +00 0.00000E+00 0.00000E+00 0.00000E+00
 0.00000E+00

YCD =

0.00000E+00 0.16567E-02 0.65324E-02 0.15098E-01 0.27740E-01 0.44585E-01 0.65277E-01
 -01 0.89093E-01 0.11487E+00 0.14085E+00
 0.16454E+00 0.21374E+00 0.26066E+00 0.28957E+00 0.28939E+00 0.24645E+00 0.19836E+00
 +00 0.15831E+00 0.12542E+00 0.98769E-01
 0.77393E-01 0.60398E-01 0.46983E-01 0.36453E-01 0.28226E-01 0.21821E-01 0.16848E-01
 -01 0.12996E-01 0.10017E-01 0.77166E-02
 0.59417E-02

SURFACE HC MASS FRACTION (YFS)

0.59588E+00 0.55527E-01 0.41276E-01 0.33799E-01 0.28303E-01 0.23840E-01 0.20075E-01
 -01 0.16396E-01 0.12835E-01 0.94545E-02
 0.63485E-02

YCD(SURFACE) =

0.00000E+00 0.12246E-03 0.40424E-03 0.86451E-03 0.15176E-02 0.23790E-02 0.34733E-02
 -02 0.47282E-02 0.60816E-02 0.74420E-02
 0.86843E-02

XJH

0.42719E+02 0.39692E+01 0.33866E+01 0.31814E+01 0.30823E+01 0.30479E+01 0.30827E+01
 +01 0.31189E+01 0.31556E+01 0.31922E+01
 0.32283E+01

EFFICIENCY (CARBON-BALANCE)

0.00000E+00 0.23405E+00 0.33119E+00 0.40983E+00 0.47854E+00 0.54072E+00 0.59893E+00
 +00 0.65439E+00 0.70766E+00 0.75908E+00
 0.80872E+00 0.83963E+00 0.86864E+00 0.89865E+00 0.92571E+00 0.94197E+00 0.95330E+00
 +00 0.96273E+00 0.97047E+00 0.97674E+00
 0.98178E+00 0.98578E+00 0.98894E+00 0.99142E+00 0.99335E+00 0.99486E+00 0.99603E+00
 +00 0.99694E+00 0.99764E+00 0.99818E+00
 0.99860E+00

1 Report No NASA CR-165324	2 Government Accession No	3 Recipient's Catalog No	
4 Title and Subtitle Transient Catalytic Combustor Model		5 Report Date May 1981	6 Performing Organization Code
		8 Performing Organization Report No	
7 Author(s) James S. T'ien		10 Work Unit No	
9 Performing Organization Name and Address Case Western Reserve University 2040 Adelbert Road Cleveland, Ohio 44106		11 Contract or Grant No. NSG - 3230	
		13 Type of Report and Period Covered Contractor Report	
12 Sponsoring Agency Name and Address U.S. Department of Energy Office of Transportation Programs Washington, D. C. 20545		14 Sponsoring Agency Code DOE/NASA/3230-1/1	
		15 Supplementary Notes Final Report, prepared under Interagency Agreement DEAI01-77CS51040. Project Manager, D. Anderson, Aerothermodynamics and Fuels Division, NASA Lewis Research Center, Cleveland, Ohio 44135;	
16 Abstract A quasisteady-gas-phase and thermally-thin-substrate model is used to analyze the transient behavior of catalytic monolith combustors in fuel-lean operation. The combustor response delay is due to the substrate thermal inertia. Fast response is found to be favored by thin substrate, short catalytic bed length, high combustor inlet and final temperatures and, in most cases, small gas channel diameters. The calculated gas and substrate temperature time history at different axial positions provides an understanding of how the catalytic combustor responds to an upstream condition change. The computed results also suggest that the gas residence times in the catalytic bed and in the after-bed space are correlatable with the nondimensional combustor response time. The model can also perform steady-state combustion calculations; and the computed steady-state emission characteristics show good agreement with available experimental data in the range of parameters covered. From combined steady and unsteady considerations, it is possible to choose a catalytic combustor design for automotive gas turbine engine which has reasonably fast response (< 1 second) and can satisfy the emission goals in an acceptable total combustor length.			
17 Key Words (Suggested by Author(s)) Catalytic combustion Transient combustion Combustor modeling		18 Distribution Statement Unclassified - unlimited Star Category 44 DOE Category UC-96	
19 Security Classif. (of this report) Unclassified	20 Security Classif. (of this page) Unclassified	21 No. of Pages	22 Price*

* For sale by the National Technical Information Service, Springfield, Virginia 22161



3 1176 00507 3466